Master's thesis

NTNU
Norwegian University of Science and Technology
Faculty of Medicine and Health Sciences
Department of Clinical and Molecular Medicine

Synne-Louise Trøen

Exploring cell death mechanisms upon infection with respiratory syncytial virus

Master's thesis in Molecular Medicine
Supervisor: Marit Walbye Anthonsen
May 2024

NTNU
Norwegian University of
Science and Technology

Synne-Louise Trøen

Exploring cell death mechanisms upon infection with respiratory syncytial virus

Master's thesis in Molecular Medicine
Supervisor: Marit Walbye Anthonsen
May 2024

Norwegian University of Science and Technology
Faculty of Medicine and Health Sciences
Department of Clinical and Molecular Medicine

NTNU
Norwegian University of
Science and Technology

Acknowledgements

This master thesis was conducted at the Department of Clinical and Molecular Medicine (IKOM) within the Faculty of Medicine and Health Sciences at the Norwegian University of Science and Technology (NTNU) in Trondheim.

First, I am deeply grateful to my supervisor, Marit W. Anthonsen, for her invaluable guidance and support. Her dedication and passion for this field have been truly inspiring. I also owe a big thank you to Kristin Rian for her exceptional lab training and assistance. My fellow students in the same research group, Fredrik and Elisabeth, deserve a huge thank you for creating a motivating and supportive environment in the lab and office. I will forever be thankful that it was you two I got to share this year with.

Lastly, I would like to express my deepest appreciation to my family and friends, who have provided support and love throughout this challenging journey. Their belief in me has been a constant source of strength and motivation.

Synne-Louise Trøen
Meråker, May 2024

Abstract

Respiratory Syncytial Virus (RSV) poses a significant health challenge, particularly affecting the elderly, immunocompromised individuals, and young children. Acute lung injury induced by viruses is linked to cell death and release of the cytokine interleukin-1β (IL-1β), which attracts immune cells and may also stimulate fibrosis in the lungs. How cell death and IL-1β secretion is regulated by RSV is poorly understood. This study explores the cell death mechanisms upon infection with RSV in human lung fibroblasts (WI-38).

Our findings demonstrate that RSV infection induces lytic cell death characterized by significant lactate dehydrogenase (LDH) release, differing in its intensity magnitude when compared to HEp-2 cells, which points to a cell-type specific response to viral cytotoxicity. Alongside lytic cell death, there was an increase in RSV-induced IL-1β production, suggesting inflammasome activation, partly through the NLRP1 pathway, indicated by differential responses to specific pathway inhibitors.

Furthermore, RSV infection led to considerable DNA damage, as evidenced by increased γH2AX protein levels, a marker for DNA double-strand breaks. This was accompanied by a marked activation of the cyclic GMP-AMP synthase-stimulator of interferon genes pathway (cGAS-STING), possibly reflecting its role in sensing cytosolic DNA. The study also showed that the ATM inhibitor decreased the expression of RSV-induced RSV fusion protein levels and gave high IL-1β release, suggesting a significant interplay between the viral infection and the host's DNA damage response mechanisms.

In summary, our findings indicate that RSV not only disrupts cellular integrity through lytic processes and DNA damage responses but may also trigger inflammasomes. Exploring these interactions provides a deeper understanding of pathogenic mechanisms of RSV and offers potential pathways for targeted therapeutic interventions to reduce the adverse effects of RSV infections in lung tissue.

Sammendrag

Respiratorisk syncytialt virus (RSV) utgjør en betydelig helseutfordring, og rammer spesielt eldre, immunkompromitterte individer og små barn. Akutt lungeskade indusert av virus er knyttet til celledød en frigjøring av cytokinet IL-1β, som tiltrekker immunceller og kan også stimulere fibrose i det lange løp. Hvordan celledød og IL-1β-sekresjon reguleres av RSV er lite utforsket. Denne studien utforsker celledødsmekanismene ved infeksjon med RSV i humane lungefibroblaster (WI-38).

Våre funn viser at RSV-infeksjon induserer lytisk celledød karakterisert ved frigjøring av laktatdehydrogenase (LDH), som er høyere i WI-38 celler, sammenlignet med HEp-2-celler, noe som peker på en celletypespesifikk respons på viral cytotoksisitet. I tillegg til lytisk celledød var det en økning i RSV-indusert interleukin-1β (IL-1β) produksjon, noe som tyder på inflammasomaktivering, delvis gjennom NLRP1-signalveien, indikert av ulike responser på spesifikke hemmere.

Videre førte RSV-infeksjon til betydelig DNA-skade, som ble bekreftet av økte γH2AX-proteinnivåer, en markør for DNA-dobbeltrådsbrudd. Dette ble fulgt av en markert aktivering av den cytosoliske DNA sensoren sykliske GMP-AMP-syntase (cGAS) - stimulator av interferon-gener (STING), cGAS-STING-signalveien, som muligens gjenspeiler dens rolle i sensing av cytosolisk DNA. Studien viste også at ATM-hemmer reduserte uttrykket av RSV-induserte RSV-fusjonsproteinnivåer og ga høy IL-1β-frigjøring, noe som tyder på et betydelig samspill mellom virusinfeksjonen og vertens DNA-skaderesponsmekanismer.

Oppsummert indikerer funnene våre at RSV ikke bare forstyrrer cellulær integritet gjennom lytiske prosesser og DNA-skaderesponser, men kan også utløse inflammasomer. Utforsking av disse interaksjonene gir en dypere forståelse av RSV sine patogene mekanismer og tilbyr potensielle veier for målrettede terapeutiske intervensjoner for å redusere de negative effektene av RSV-infeksjoner i lungevev.

Abbreviations

ASC: Apoptosis-associated speck-like protein containing a CARD

CARD: Caspase activation and recruitment domain

cGMAP: Cyclic guanosine monophosphate-adenosine monophosphate

cGAS: Cyclic GMP-AMP synthase

DMEM: Dulbecco's Modified Eagle's Medium

DMSO: Dimethyl sulfoxide

dsDNA: Double-stranded DNA

dsRNA: Double-stranded RNA

ELISA: Enzyme-linked immunosorbent assay

FBS: Fetal bovine serum

HMW: High molecular weight

HPV: Human Papilloma Virus

HMW p(I:C): High molecular weight poly(I:C)

IFN: Interferon

LDH: Lactate dehydrogenase

NF-κB: Nuclear factor kappa B

NLR: NOD-like receptor

NLRP: NLR family, PYD domain containing

PAMP: Pathogen-associated molecular patterns

PBS: Phosphate buffered saline

Poly(dA:dT): Poly(deoxyadenylic-deoxythymidylic) acid sodium salt

Poly(I:C): Polyinosine-polycytidylic acid

PRR: Pattern recognition receptor

qPCR: Real-time quantitative PCR

qRT-PCR: Quantitative real-time polymerase chain reaction

STING: Stimulator of interferon genes

TLR: Toll like receptor

TNF: Tumor necrosis factor

Table of content

1 Introduction

1.1 Viral infections

Viral infections initiate when a virus successfully enters the host and begins to replicate within host cells (1). This intrusion activates the host's immune response, which is a multi-faceted defense system involving both innate and adaptive components (2, 3). Common viral infections include influenza virus, rhinovirus, SARS-COV-2, human papillomavirus (HPV), and the herpes simplex virus (HSV) (4). These viruses are responsible for a significant global health burden, with influenza and SARS-COV-2 being notable for their potential to cause seasonal epidemics and global pandemics (5, 6). There is a continuous need for research to address the challenges posed by these viruses and to develop effective viral treatments.

1.2 Immune response to viral infections

Immune responses are the body's mechanisms to react to, identify, control, and eliminate viral pathogens (7). These responses trigger a wide range of actions and involve the innate- and adaptive immune system (7). The first line of defense is the innate immunity and this is activated immediately following infection and employs general defense strategies such as inflammation and fever (8). Innate immunity also includes the recruitment of immune cells like macrophages and dendritic cells to the site of infection (9). These cells are crucial for capturing viral antigens and presenting them to lymphocytes, thereby linking innate and adaptive immune responses (9). The innate system’s rapid response is mediated through pattern recognition receptors (PRRs) that detect viral pathogen-associated molecular patterns (PAMPs) (10, 11).

Following the innate response, the adaptive immune system takes over with a more specific and refined response (7). The adaptive immune response is divided into two branches, humoral- and cellular immunity (7). Humoral immunity involves B cells that produce antibodies (7). Antibodies are proteins which recognize and binds antigens, while antigens are molecules from pathogens, like virus (7). The antibodies will bind to these and neutralize them or mark the for destruction by other cells of the immune system (7, 9). The other branch is the cellular immunity, which involves T cells(7). There are several types of T cells, including helper T cells, which aid other immune cells; cytotoxic T lymphocytes (CTLs), which kill infected cells; and regulatory T cells, which help modulate the immune response to

avoid attacking self-tissues (7, 12). Together, the innate and adaptive immune responses are fundamental in preserving health and providing a robust defense against infections (7).

1.3 The role of cytokines in antiviral immunity

Cytokines play a crucial role in coordinating an antiviral defense by initiating inflammation and mobilizing immune cells, such as macrophages and dendritic cells, to the site of infection, thereby enhancing the body's ability to combat viruses (13). Cytokines consists of groups such as interleukins (IL-), interferons (IFN) and tumor necrosis factors (TNF) (13, 14). Interferons, a subset of cytokines are important in our body due to their antiviral roles (15). There are several types of interferons, including Type I (IFN-α and IFN-β), Type II (IFN-γ), and Type III (IFN-λ), each with distinct biological activities and roles in immune regulation (15, 16). Type I interferons, specifically IFN-α and IFN-β, are critical cytokines produced by cells in response to viral infections (15, 17). Upon detection of viral components, these cells activate Type I interferons that bind to interferon alpha/beta receptors (IFNAR) on neighboring cells (15, 17). This interaction induces the expression of interferon-stimulated genes (ISGs), enhancing the antiviral defenses by interfering with viral replication and spread (15, 17). The activation of ISGs not only enhances the innate immune response but also modulates the adaptive immune system, ensuring a robust and coordinated defense (15, 17). This dual action significantly amplifies the body's capacity to combat viral infections, illustrating the integrated roles of innate and adaptive immunity (18, 19).

1.4 Respiratory syncytial virus

Respiratory syncytial virus (RSV), part of the Paramyxoviridae family, is a negative single-stranded, enveloped RNA virus (20). It primarily poses a significant health risk to the elderly, infants, and individuals with compromised immune systems (21, 22). Although many infected with RSV only exhibit mild cold-like symptoms, the virus can lead to severe respiratory illness in vulnerable groups such as the elderly, immunocompromised individuals, and children under five years of age, often necessitating hospitalization (23). Later in life, people infected with RSV during their childhood, have a higher risk of developing chronic lung disease (24). RSV spreads through airborne droplets and it can also be transmitted by direct contact with infected individuals or indirectly through contact with contaminated surfaces (25). The incidence of RSV infections varies seasonally, and the virus exhibits genetic diversity (22). Infections typically peak during the autumn and early winter in northern

countries, a pattern that is influenced by environmental factors such as temperature and humidity, which affect virus survival and transmission rates (26). Currently, no vaccine is available to protect against RSV (23).

To fully comprehend the pathophysiology of Respiratory Syncytial Virus (RSV), it is essential to understand both its virion structure and its replication mechanisms within host cells (Figure 1). The virion of RSV is characterized by a lipid envelope that surrounds a helical nucleocapsid, which contains the negative-sense, single-stranded RNA genome (27). The genome of RSV is approximately 15.2 kilobases (kb) in length and encodes 11 proteins, including structural and non-structural proteins that play critical roles in the virus's life cycle and in modulating the host's immune response (27, 28).

Upon entering the host cell, RSV can use two primary methods for cellular entry: direct fusion of the viral envelope with the plasma membrane or receptor-mediated endocytosis leading to the release of the virus into endosomes (28). Once inside, the viral envelope merges with the endosomal membrane, or directly with the cell membrane, allowing the nucleocapsid to enter the cytoplasm (28).. This event triggers the disassembly of the viral components to form what is known as a polymerase complex (Figure 2) (28). This complex, containing the viral RNA, RNA-dependent RNA polymerase, and other viral proteins, is crucial for initiating the replication of the viral genome within the cytoplasm of the infected cell (28).

The replication process involves the synthesis of viral mRNA from the viral RNA template—a process known as transcription (28). The viral mRNA is then used to produce viral proteins necessary for assembling new virions (28). Concurrently, the polymerase complex also synthesizes full-length, positive-sense RNA copies of the genome (28). These serve as templates for producing additional negative-sense viral RNA, thereby completing the replication cycle (28). The newly formed viral genomes and structural proteins are then assembled into new virions, which are eventually released from the cell by budding, taking portions of the host cell membrane as their new envelopes (28).

Understanding these detailed interactions and processes is vital for studying how RSV triggers disease processes within the body, influencing the development of targeted therapies and interventions.

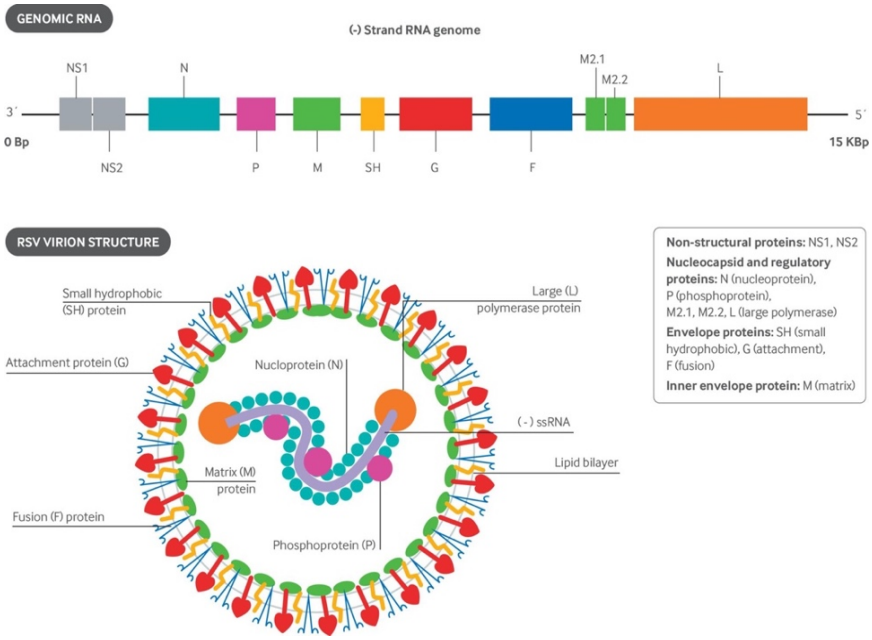

Figure 1. Genomic RNA and RSV virion structure. The genomic RNA sequence and the virion's structural composition. Genomic RNA: RSV is a negative-strand RNA genome, showing nonstructural proteins NS1 and NS2 at the 3' end, followed by the nucleocapsid N protein, phosphoprotein P, matrix M protein, small hydrophobic SH protein, attachment G protein, fusion F protein, regulatory proteins M2.1 and M2.2, and the large polymerase L protein at the 5' end. The genome is flanked by leader and trailer sequences that are critical for transcription and replication. The G protein varies between RSV A and B, while F protein is conserved and induces broad immunity – being a potent vaccine antigen. RSV virion structure: Shows the arrangement of structural proteins in the lipid bilayer. The G protein is responsible for virus attachment to host ciliated cells, F protein facilitates membrane fusion and entry, and the SH protein, which functions as a viroporin, together they play critical roles in RSV infectivity. Figure adapted from (27).

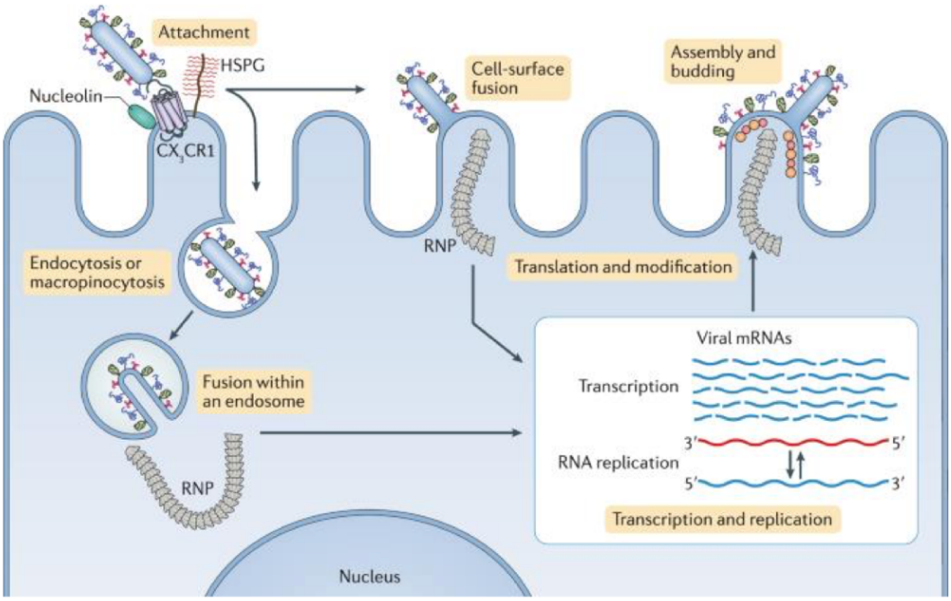

Figure 2. RSV infection cycle. This shows how the RSV infection process is in ciliated epithelial cells, starting with virion attachment through the G glycoprotein to cell surface HSPG. Viral entry follows, facilitated by the F glycoprotein, which enables membrane fusion and RNP release into the cytoplasm. Here, transcription and

genome replication occur, driven by the viral RdRp in inclusion bodies (not shown in figure). Virion assembly takes place near the plasma membrane, leading to budding and release of filamentous virions. Over time, these can transform into less infectious spherical particles due to changes in the matrix (M) protein (shown in orange by the RNP at top right) and fusion (F) protein conformation (connected to the M-protein in figure). Figure adapted from (28).

1.5 Immune response to respiratory syncytial virus

Respiratory Syncytial Virus (RSV) triggers a complex immune response involving both the innate and adaptive immune systems (29). Upon infection, RSV is detected by various pattern recognition receptors (PRRs), including Toll-like receptors (TLRs), RIG-I-like receptors (RLRs), and nucleotide-binding oligomerization domain-like receptors (NLRs) (29). These receptors initiate immune signaling cascades that produce type I and III interferons (IFNs) and other cytokines, crucial for the antiviral defense (29). This response is orchestrated through adaptor proteins like MAVS and TRIF, activating transcription factors such as interferon regulatory factor 3 (IRF3) and nuclear factor kappa B (NF-κB), which amplify the transcription of genes encoding interferons and inflammatory mediators (18, 29, 30).

RSV has developed sophisticated mechanisms to evade these immune responses, enhancing its virulence and ability to cause recurrent infections (31). Critical to this evasion are the RSV proteins NS1 and NS2, which suppress the production of IFN-α and IFN-β, key components of the host's antiviral response (32). Moreover, RSV can disrupt the balance of the adaptive immune system, leading to insufficient T-cell memory and suboptimal antibody production, thereby complicating efforts to control infections (33). Such immune evasion strategies can result in a lack of durable immunity, frequent re-infections, and can exacerbate other respiratory conditions (33). In severe cases, such as bronchiolitis in infants, RSV-driven immune responses can lead to significant tissue damage, characterized by increased mucus production and airway obstruction (34, 35). Understanding these complex immune dynamics is crucial for developing effective strategies to mitigate the impact of RSV, particularly among vulnerable populations. Given the substantial immune evasion facilitated by RSV, particularly through mechanisms that weaken both innate and adaptive immune defenses, the body's resultant cellular stress and damage are significant, and may lead to cell death.

1.6 Cell death mechanisms

Cell death mechanisms such as apoptosis, necrosis, and pyroptosis are critical biological processes that respond to cellular stress and damage (36). Apoptosis is a form of programmed

cell death, that ensures the removal of cells without eliciting an inflammatory response (37). In contrast, necrosis refers to uncontrolled process resulting from external damage to the cell or tissue, often leading to cell swelling, bursting and subsequent inflammation, damaging surrounding cells (36, 38). Pyroptosis, another form of programmed cell death, is inherently inflammatory and crucial for immune responses as it releases cytokines and inflammatory signals, alerting the immune system to infection (39, 40). Despite the different distinct pathways and outcomes of these cell death mechanisms, they share fundamental roles in disease progression, immune response, and tissue homeostasis (41). Lytic cell death, a broader term, encompasses various specific forms of cell death, including necroptosis and pyroptosis (42). Lytic cell death specifically describes cell death resulting in the cell bursting and releasing its contents and can be measured by lactate dehydrogenase assay (LDH) (22).

Central to these inflammatory responses is interleukin-1β (IL-1β), a pro-inflammatory cytokine that is instrumental in regulating immune reactions to infections (43). IL-1β originates as a biologically inactive precursor, pro-IL-1β, which is produced within cells as part of an inactive complex (44). For activation, pro-IL-1β requires processing by caspase-1, transitioning from its inactive precursor form to an active cytokine that amplifies the immune response during events like pyroptotic cell death (40, 44). Additionally, reactive oxygen species (ROS) play a significant role in modulating both pyroptosis and necroptosis (45). These molecules enhance the complexity of cellular responses to damage and infection, indicating their double-edged roles in various biological processes (46).

1.7 Caspases: Key regulators of cell death and inflammation

Caspases, a family of protease enzymes, are pivotal in mediating programmed cell death and inflammation (47). Caspases are initially synthesized as inactive precursors called zymogens or procaspases and become activated through proteolytic cleavage triggered by various intra- and extracellular signals (47). Caspase-1, essential for the inflammatory response, activates pro-inflammatory cytokines like IL-1β and interleukin-18 (IL-18) through inflammasomes in response to pathogens or stress (44, 48). Caspase-3, known as the principal executioner in apoptosis, is activated downstream by caspase-8 and caspase-9, leading to the breakdown of cellular components and ultimately cell death . Together with caspase-6 and caspase-7, which also play roles in apoptosis, these caspases illustrate a complex network of proteolytic enzymes that regulate critical processes of cell death and immune response (49). In contrast, caspase-1 is activated by inflammasomes, caspase-3 is activated by other caspases, i.e.

capsase-8 and -9. Caspase-1 and caspase-3 follows pyroptotic and apoptotic stimuli, respectively (50, 51).

The balance between the activity of caspases is vital for the proper functioning of the immune response and maintenance of tissue homeostasis (52). Dysregulation of caspase activity is associated with a variety of diseases, including autoinflammatory conditions, cancer, and neurodegenerative disorders (49). Because of their crucial roles, caspases are also interesting targets for therapeutic interventions. It is shown, in mice, that targeted deletion of caspase-3 can be useful in limiting cell death in conditions such as myocardial infarction (53).

Research suggests that RSV infection triggers ER stress and mitochondrial damage, enhancing viral replication through increased mitochondrial ROS production (54). This viral strategy might involve caspase activation to suppress interferon production, potentially benefiting the viral lifecycle by weakening the host's immune defense (55). Consequently, targeting caspase inhibition could potentially enhance interferon responses and impair RSV proliferation, representing a promising therapeutic approach (56). Moreover, the interaction between viral activation of caspases and inflammasome pathways underscores a complex regulatory network that may amplify inflammatory and immune responses during RSV infections (56, 57). Central to the immune system’s response to pathogens, these inflammasome complexes detect viral acitvites and cellular stress, ultimately triggering caspase-1 activation (57, 58).

1.8 Inflammasome structure and function in immune response

Inflammasomes are multiprotein complexes, NLRP1 was the first identified inflammasome in 2002 by Martinon et al., and plays a vital role in the immune response to viral pathogens (59). Inflammasomes regulate inflammation and mediate pyroptosis, a type of programmed cell death distinct from the apoptosis regulated by caspases such as caspase-3 (49). Inflammasomes detect cellular damage and activate inflammatory responses, integrating signals that lead to the activation of caspase-1 (60). Common components of NLRP1 and NLRP3 inflammasomes include a pyrin domain (PYD), a nucleotide-binding and oligomerization domain (NACHT), and leucine-rich repeats (LRR) at the C-terminal end (Figure 3) (61, 62). NLRP1 also features a FIIND domain, comprising ZU5 and UPA segments, and a caspase recruitment domain (CARD) at its C-terminal (Figure 3) (61, 62).

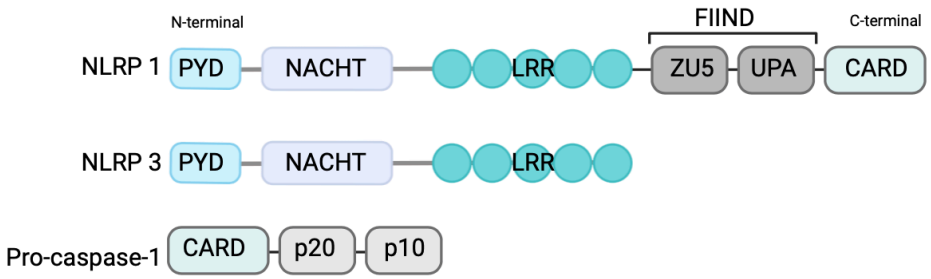

Figure 3. Structure of NLRP1, NLRP3 and pro-caspase-1. The figure illustrates the domain structures of key inflammasome proteins, each depicted with color-coded domains to emphasize their structural and functional features. N-terminal and C-terminal side of the molecules are indicated. NLRP3 and NLRP1 from the NLR family feature a PYD, NACHT, and LRR domain, with NLRP1 also including FIIND (ZU5, UPA), and CARD domains for enhanced functionality. Pro-caspase-1 is characterized by a CARD domain and catalytic p20 and p10 subunits, they are important in sensing stress or pathogens, initiating assembly, and driving the inflammatory response. Figure created with Biorender (www.biorender.com).

NLRP1, the first identified member of the NLR protein family, plays a crucial role in forming a cytosolic inflammasome that is essential for the activation of caspase-1 and the subsequent inflammatory response (59). In humans, NLRP1 activation involves a unique autoproteolytic process, which is vital for its function in diseases affecting epithelial barriers (63). This inflammasome is activated in mouse macrophages, but human NLRP1 is found mostly in keratinocytes and bronchial epithelial cells (63-65). ValBoro Pro (VBP), which is a NLRP1 inducer, is shown to trigger the release of IL-1β and LDH release in a variety of cells (22, 66, 67). The intricate mechanisms of NLRP1 activation and its regulation not only underscore its significance in inflammation but also present it as a potential target for therapeutic interventions in related diseases (68).

NLRP3 is extensively studied due to its pivotal role in immune responses against viral infections. It is primarily expressed in myeloid cells, such as monocytes, dendritic cells, macrophages, and neutrophils, and is also found in epithelial cells (68-70). This broad distribution highlights its crucial function in orchestrating immune defenses across various tissues (71). Additionally, during viral infections, both NLRP1 and NLRP3 are critical in inducing the formation of the inflammasome, a key process in initiating an effective inflammatory response to control and eliminate the viral threat (22).

NLRP1 and NLRP3 differ in their activation mechanisms and the signals they respond to. NLRP1 can be activated directly by pathogen-derived molecules and by certain toxins that

induce proteasome activity (63). NLRP1 includes a function-to-find domain (FIIND) and a CARD domain that are not found in NLRP3, enabling it to directly recruit and activate caspase-1 (72). Unlike NLRP1, NLRP3 responds to a broader range of signals, mainly involving cellular stress and damage such as potassium efflux, reactive oxygen species (ROS), and lysosomal disruption (73). NLRP3 activation requires the adaptor protein ASC and pro-caspase-1 to form a complex for caspase-1 activation (73). These differences affect how each inflammasome contributes to immune responses, with NLRP3 being more broadly involved in responding to cellular stress signals compared to the more direct pathogen detection mechanisms of NLRP1 (74, 75). A general inflammation activation-pathway is shown in figure 4.

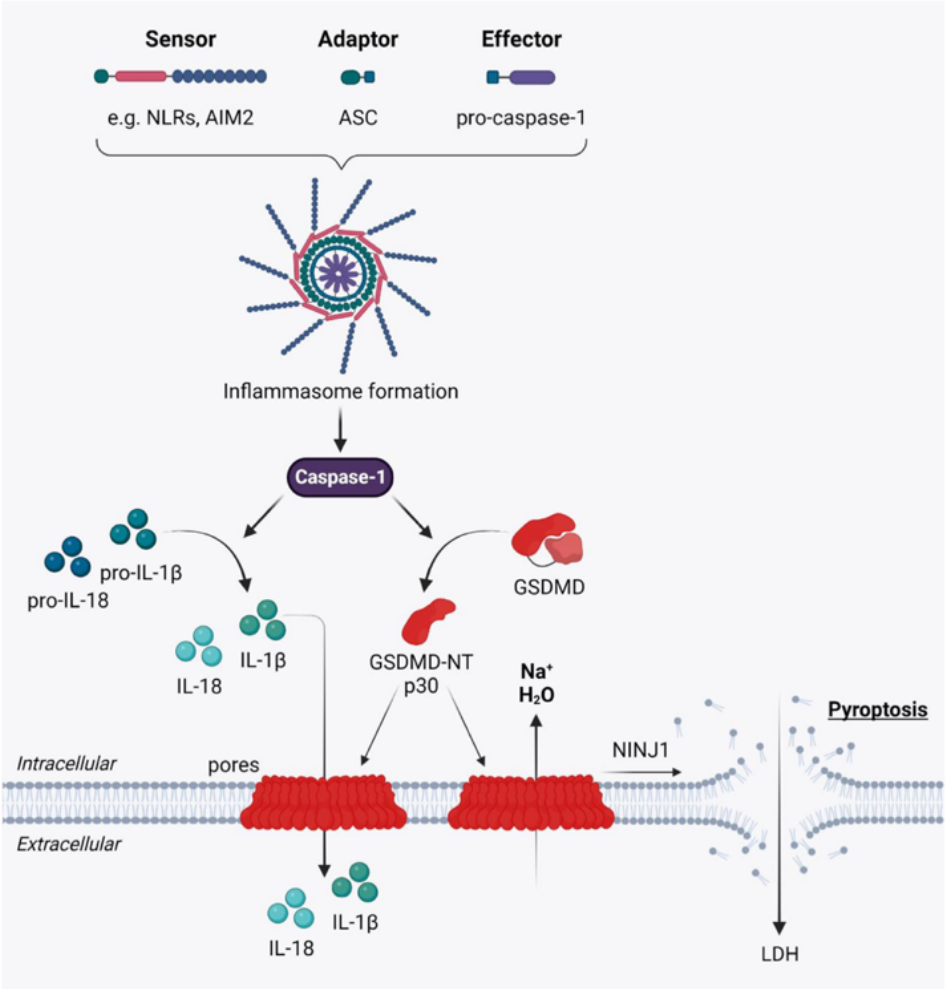

Figure 4. Inflammasome activation and pyroptosis. Inflammasome formation starts with cytosolic danger signals detected by pattern recognition receptors like NLRs and AIM2, which recruit the adaptor protein ASC to form the inflammasome. Within this complex, pro-caspase-1 is activated to caspase-1, cleaving pro-IL-1β and pro-IL-18 into active cytokines IL-1β and IL-18. Caspase-1 also processes gasdermin D (GSDMD), with the resulting N-terminal fragment forming membrane pores that release IL-1β and IL-18, leading to cell swelling, lysis, and the characteristic release of lactate dehydrogenase (LDH). The figure also shows ion fluxes and proteins like NINJ1 in regulating this pathway and the release of LDH. Figure adapted from (22).

1.9 The cGAS-STING pathway

The cGAS-STING pathway, comprising the cytosolic DNA-sensor cyclic GMP-AMP synthase (cGAS) and the stimulator of interferon genes (STING), is a critical DNA-sensing mechanism initially identified for its role in detecting cytosolic DNA (76). The cGAS-STING pathway is shown to be involved in SARS-COV-2- and paramyxovirus-infection (77, 78). Although the mechanisms by which this pathway interacts with RNA viruses, such as RSV, remain largely unknown, research into the STING pathway in relation to RNA viruses is expanding. This increased focus could potentially reveal how the STING pathway contributes to the control of some RNA viruses.

The cGAS-STING pathway primarily functions to detect cytosolic DNA released during viral infections, which triggers a host defense mechanism that is essential not only for combating pathogens but also for regulating several other cellular processes such as inflammation, cell death and cellular senescence (79, 80). DNA, cGAS synthesizes a second messenger, cyclic GMP-AMP (cGAMP), which activates STING (Figure 5) (80). This leads to the production of type I interferons and other cytokines critical for the antiviral response (13, 80). Upon activation, STING triggers several downstream signaling cascades, including the activation of transcription factors like IRF3 and NF-κB, which travel to the nucleus to stimulate the expression of immune response genes (81). This process is instrumental in initiating apoptosis through pathways such as endoplasmic reticulum (ER) stress and can influence broader immune and cellular responses to maintain cellular integrity under stress (81).

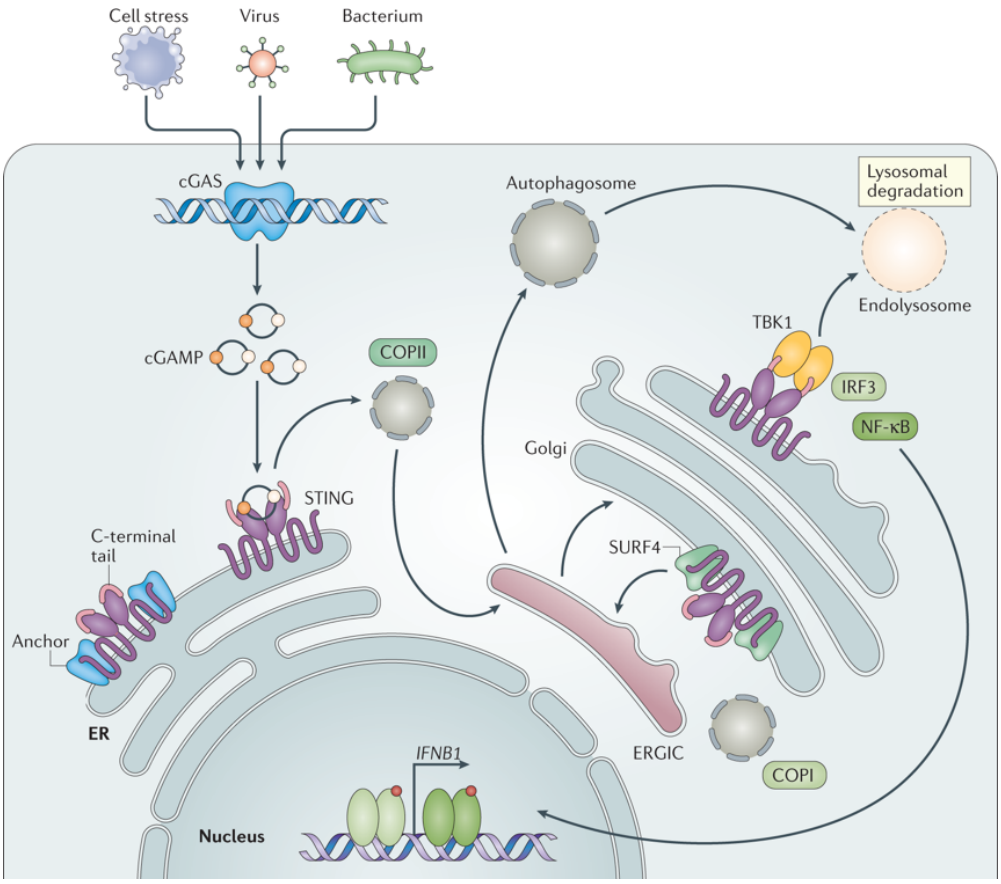

Figure 5. Activation of cGAS-STING pathway by cytosolic DNA detection. cGAS catalyzes the formation of cGAMP, activating STING, which relocates from the endoplasmic reticulum (ER) to the Golgi. This relocation triggers the activation of TBK1, leading to the activation of transcription factors such as IRF3 and NF-κB. These factors then enter the nucleus, stimulating the production of type I interferons and other immune response genes. Additionally, the figure highlights the pathway's connection to autophagy and the roles of various transport proteins in modulating the response, integrating multiple cellular processes and immune mechanisms. Figure adapted from (80).

STING plays a pivotal role in modulating cell death and the release of IL-1β (82). Activation of STING can lead to cell death through various mechanisms, including the induction of apoptosis and necroptosis (82). Specifically, STING activation promotes apoptosis by upregulating genes that initiate apoptotic pathways (83). In scenarios where cells are infected by viruses or experience severe DNA damage, STING activation can also trigger necroptosis (80). Regarding the release of IL-1β, STING activation enhances the production of type I interferons and other inflammatory cytokines, which in turn stimulate the assembly of the inflammasome complex (83, 84).

1.10 DNA damage response

The DNA damage response (DDR) is a crucial cellular mechanism that detects, signals and repairs damage in the DNA (85). The DDR consists of a network of cellular pathways,

working together to maintain genomic stability by repairing DNA (85). DNA damage can occur due to environmental factors or trough interactions with certain chemicals or radiation (86, 87). A key component of the DDR is γH2AX, the phosphorylated form of the histone protein H2AX, which acts as a critical marker for double-stranded breaks (DSB) in DNA (85, 86). Upon a DSB, H2AX is phosphorylated at the site of damage by PI3 kinase-related kinases such as ATM, ATR and DNA-PK (86, 88, 89). This phosphorylation of H2AX helps in recruiting DNA repair proteins at the site of damage, facilitating DNA repair processes (90).

Viruses are known to induce DNA damage in host cells either directly—by integrating into the host genome and disrupting normal replication processes—or indirectly through reactive oxygen species (ROS) and other byproducts that harm DNA (90, 91). Such DNA damage can lead to mutations, cellular senescence, apoptosis or other forms of cellular stress (90). If DNA damage remains unrepaired, it can result in mutations that may lead to oncogenesis or impair critical gene functions (90, 92). Further, cells may enter a state of permanent cell cycle arrest, known as senescence, which acts as a tumor suppressor mechanism (92). It may also contribute to aging and chronic diseases (92). At last, persistent DNA damage can trigger stress responses that can influence cellular metabolism, growth and apoptosis (92).

2 Aim of the study

Respiratory Syncytial Virus (RSV) is a major respiratory pathogen with significant impact on human health. Airway viruses often induce cell death related to lung injury and knowledge on how RSV interacts with cell death and cell death components is an important aspect. For understanding RSV-mediated pathogenesis the aim of this study was to explore cell death and IL-1β release induced by RSV in relevant human cells, and to evaluate the involvement of components known to regulate IL-1β secretion to other stimuli. This study focuses on the characterization of RSV infection in HEp-2 and WI-38 cells. We examined that RSV influences cell death, IL-1β release and DNA damage marked by γH2AX. Additionally, we compare the effect of RSV on cellular outcomes against those triggered by synthetic analogs like poly(dA:dT) (p(dA:dT)), poly(I:C) (p(I:C)), and ABT737, a Bcl-2 and Bcl-xL inhibitor. A key aim is to assess the impact RSV have on caspase-1 activity and its interaction with NLRP1 inflammasomes, critical components of the inflammatory response. The following aims were conducted in this thesis:

- Explore the ability of RSV to influence cell death and IL-1β release in HEp-2 and WI-38 cells.
- Evaluate the ability of cells to express mRNA of NLRP3 and NLRP1
- Determine if RSV affect mRNA and protein levels of NLRP3- or NLRP1 inflammasomes in HEp-2 and WI-38 cells.
- Explore the role of caspases in RSV-induced IL-1β release and activation of caspase-1 by RSV in WI-38 cells.
- Determine the effect of RSV to induce DNA damage in WI-38 cells.
- Explore the impact of a STING inhibitor on RSV-induced IL-1β release in WI-38 cells.

3 Methodology

3.1. Maintaining and seeding HEp-2 and WI-38 cells

Throughout this project, both HEp-2 and WI-38 cells were cultivated. HEp-2 cells were provided from Erasmus Medical Center in Rotterdam, by B. van den Hoogen. HEp-2 cells were cultured in Dulbecco's Modified Eagle Medium (DMEM) (Sigma-Aldrich #D6429), adding 10% Fetal Bovine Serum (FBS) (Sigma-Aldrich #F7436) and 1% Penicillin-Streptomycin (Pen-Strep) (Gibco, #15070063) and 0,7 mM L-Glutamine (#G7513, Sigma-Aldrich) to the DMEM. Wi-38 cells were obtained from Sigma-Aldrich (#90020107) and were cultured in DMEM, adding 10% FBS and 1% Pen-Strep. FBS enriches culture media with vital nutrients and supports cell growth and adhesion, while maintaining pH stability (93). L-glutamine is added to cell culture media as a crucial nutrient for growth and energy, while Pen-Strep works against bacterial contamination. Both cell lines were maintained at 37°C in a 5% CO2 atmosphere and sub-cultured when reaching approximately 80% confluency.

Subculturing involved rinsing the cells with 1X phosphate buffer saline (PBS) (Gibco, #18912014) and detaching them from the cell flask using Trypsin-EDTA (Sigma-Aldrich #T3924). Excess trypsin was removed by centrifuging the cells at 1500 rpm for 5 minutes, forming a cell pellet. This pellet was then resuspended in medium, preparing the cells for counting. The final step involved seeding the cells into new flasks for further growth or for initiating new experiments.

Cells were subsequently split into 75 cm^2 flasks for further growth or plated according to the specific requirements of the given experiment. For the LDH assay, both HEp-2 and WI-38 cells were seeded at a density of 8,000 cells per well in a 96-well plate. In the case of Western Blotting (WB), HEp-2 cells were plated at 80,000 cells per well, while WI-38 cells were at 70,000 cells per well in 24-well plates. For quantitative PCR (qPCR) analysis, HEp-2 cells were seeded at 40,000 cells per well, and WI-38 cells at 35,000 cells per well in 48-well plates. Additionally, for the active caspase-1 assay, WI-38 cells were seeded at 140,000 cells per well in 12-well plates.

3.2. *In vitro* RSV infection

To prepare for in vitro RSV infection, cells were appropriately seeded in the designated wells and quantities specific to each experiment. Both cell lines were infected with the RSV A2 strain at a multiplicity of infection (MOI) of 3 in serum reduced medium OptiMEM (Gibco, #31985047) supplemented with 2% FBS and 0,3 % L-glutamine. The RSV A2 strain was obtained from Erasmus Medical Center in Rotterdam, courtesy of B. van den Hoogen. Laboratory personnel propagated the RSV strain in HEp-2 cells, preparing the virus for subsequent in vitro infection experiments with both cell lines involved in this study. The incubation period for the infected cells ranged from 12 to 72 hours, as detailed in the results section.

3.3. Inhibitors and inducers

A various of inhibitors and activators were utilized in this thesis. Both inhibitors and activators are used in research by either activating, blocking, or modulating different targets. The inhibitors used were ABT737 (MCE #HY-50907), STING inhibitor C-171 (Selleckchem #E0128), Q-VD-OPh (MCE #HY-12305), Belnacasan (VX765) (MCE #HY-13205), ADS032 (MCE #HY-156798), and three enzyme inhibitors, ATMi (MCE #HY-12016), ATR inhibitor (MCE #HY-19323) and PARP inhibitor (MCE #HY-13688A). ValBoro Pro (InvivoGen #tlrl-vbp-10) were used as an inducer. Cells were pre-incubated with the inhibitors for 30-35 minutes before RSV infection. There was a variety of concentrations and duration used for the inhibitors and inducers as indicated in result section.

3.4. Transfection of poly(dA:dT) and poly(I:C)

Prior to transfection, cells were seeded in appropriate culture plates depending on which analysis should be done. For the mock control, Lipofectamine® 2000 (Invitrogen #11668-027) was diluted in MQ-water and further diluted in Opti-MEM Reduced Serum Medium (Invitrogen) to the final concentration as indicated in the results section. p(dA:dT) or p(I:C) was diluted in Opti-MEM, and Lipofectamine 2000 was added, and incubated in room temperature for at least 10 min. After transfection, the transfection mix added to the wells, and they were further incubated for 24-48 hours. The used concentrations of p(dA:dT) and p(I:C) is indicated in the results section.

3.5. RNA isolation and CDNA synthesis

RNA isolation is a process designed to extract RNA from a sample. When cells are harvested, a mixture of RLT buffer (Qiagen, #172041951) with 1% β-mercaptoethanol (Sigma, #M3148) is utilized. This combination is effective in minimizing RNA degradation and maximizing the quality of the RNA isolated. The isolation of total RNA is performed in accordance with the manufacturer's instructions, included the DNase digestion step, using the RNeasy Mini kit (Qiagen, #74104). To prepare for further analysis, it is important to measure the RNA concentration and purity; this is accomplished using a NanoDrop ND-1000 Spectrophotometer (Saveen Werner).

Preparing for cDNA synthesis requires having already isolated the RNA. The next critical step is converting RNA into DNA, facilitating further analyses such as RT-qPCR. This conversion is achieved using a qScript cDNA synthesis kit (Quantabio, #95047-100), with the process carried out in a thermal cycler (Techne CT-512). The thermal cycler program includes: 1 cycle at 22°C for 5 minutes, 1 cycle at 42°C for 30 minutes, 1 cycle at 85°C for 5 minutes, followed by a hold at 4°C. This protocol ensures efficient reverse transcription of RNA into cDNA.

3.6. Real time quantitative polymerase chain reaction (RT-qPCR)

Real-time quantitative PCR (qPCR) is a molecular technique used to amplify and concurrently quantify target DNA sequences. For RNA quantification, the initial step involves reverse transcription to convert RNA into complementary DNA (cDNA). This cDNA then serves as the template in the qPCR assay, which employs fluorescent markers—such as SYBR Green—to monitor the accumulation of the amplified product in real time. The specificity of amplification is governed by primer sets designed to anneal to unique sequences within the target DNA (94).

The PCR amplification process itself consists of cyclic temperature fluctuations, comprising: (Step 1) Denaturation, where the sample is heated to approximately 95°C to separate the DNA strands; (Step 2) Annealing, where the temperature is lowered to enable primer binding to the now single-stranded DNA, with the precise temperature tailored to the primer's melting point; and (Step 3) Elongation, occurring at around 72°C, where DNA polymerase extends the primers to form a new strand of DNA. This process is cyclically repeated, typically for 40 cycles, doubling the amount of the target DNA region with each cycle (94).

The qPCR was conducted in technical triplicates across 96-well plates using the StepOnePlus™ Real-Time PCR System (Applied Biosystems™). The cycling conditions were set to an initial denaturation at 95°C for 20 seconds, followed by 40 cycles of 95°C for 3 seconds and 65°C for 30 seconds each. After the PCR cycle, there will be an amplification plot from each primer used in the set-up, this shows the amount of fluorescence emitted by the reporter dye, which is proportional to the amount of PCR product (amplicon) generated during each cycle of the PCR process (94). The expression levels were calculated using the comparative ΔΔCT method in Excel, with GAPDH serving as the reference gene for normalization. The resulting C_T values, ΔC_T, and fold changes (calculated as $2^{-\Delta\Delta CT}$) are presented in this thesis. Details on primer sequences are included in the supplementary S.1 Table S1.

3.7. Western blot

Western blotting, also known as immunoblotting, is a widely used technique for detecting and quantifying specific proteins in a sample. This method involves separating proteins by their molecular weight (expressed in kilodaltons, kDa) via gel electrophoresis, transferring them onto a membrane, and identifying them using primary and secondary antibodies. The secondary antibody, often tagged with a fluorescent or chemiluminescent label, emits detectable wavelengths of light, which are captured using an imaging system.

After undergoing various treatments and incubation periods as specified in the different experimental setups, the cells were subsequently lysed with lysis buffer. Lysis buffer (components listed in supplementary table S4), and further supplied with PIC (phosphatase inhibitor cocktail) 2 (Sigma-Aldrich #P5726) and -3 (Sigma-Aldrich #P0044) and Complete ™ EDTA-free protease inhibitor cocktail (Sigma-Aldrich #1183617000). After lysis the samples could be stored in -20°C freezer for future use.

Cell lysates were centrifuged at 4°C for 5 minutes, this was to remove cell debris. Next was to add NuPage LDS sample buffer (4X) (Invitrogen #NP0007) supplied with DTT (dithiohreitol 0,05M) to new Eppendorf tubes supplied with the supernatant from the cell lysate. Samples were heated on heat block at 70°C for 10 minutes with 500 rpm shaking. Short spin to collect the sample. 4-12% NuPage Bis-Tris 10 wells gel (Invitrogen #NP0321BOX) were used for gel electrophoresis run. Depending on the required molecular weight separation, either 1X

MOPS (Invitrogen, #NP0001) or 1X MES (Invitrogen #NP0002) running buffers were utilized. They were run for approx. 1 hour at 200V. SeeBlue™ Plus 2 pre-stained protein standard (Invitrogen #LC5925) and Magic Mark™ western protein standard (Invitrogen #LC5602) was added to work as ladders for protein sizes.

After electrophoresis, proteins were transferred from the gel to a nitrocellulose membrane using either the iBlot®2 Gel Transfer Device (Invitrogen) or the Trans-Blot® Turbo™ Transfer System (BioRad). The transfer procedures were carried out according to the manufacturer's instructions. For the iBlot®2 system, iBlot Mini Transfer Stacks (Invitrogen #IB23002) were used with the P0 program, which includes 1 minute at 20V, followed by 4 minutes at 23V, and 2 minutes at 25V. For the BioRad system, 0.2 µm Mini nitrocellulose transfer packs (Bio-Rad #1704158) were employed, with either the 'Mixed MW' program at 24V for 7 minutes or the 'High MW' program at 24V for 10 minutes.

After the dry-blotting step, the membrane was rinsed with 1X TBS (Tris-Buffered Saline). To minimize nonspecific antibody binding, it was then blocked using Intercept® (TBS) Blocking Buffer (LI-COR #927-60001) for one hour. Subsequently, the membrane was washed three times for 5 minutes each with 1X TBST (TBS + 0.1% Tween-20) (TBS and TBST components detailed in supplementary Table S5). The primary antibody (Supplementary Table S2) was applied, and the membrane was incubated overnight at 4°C with gentle agitation. The following day, the membrane underwent three 5-minute washes with TBST, followed by a 1-hour incubation with a complementary secondary antibody (Supplementary Table S3). After this, the membrane was washed twice for 5 minutes with TBST and then rinsed for 10 minutes with TBS. It was left to dry for at least 30 minutes before imaging. Detection and quantitative analysis were performed using a LI-COR Odyssey Imager, and band intensity, proportional to protein concentration, was quantified using Image Studio version 5.2 software.

3.8. LDH assay

Cellular cytotoxicity was assessed using the CyQUANT™ LDH Cytotoxicity Assay (Invitrogen, #C20300). This colorimetric assay quantifies lactate dehydrogenase (LDH) release, an indicator of cell membrane damage and cell death. LDH catalyzes the conversion of lactate to pyruvate, which, coupled with the reduction of NAD+ to NADH, reduces a tetrazolium salt (INT) to a red formazan product. The intensity of this product, measured

with FLUOstar omega microplate reader (BMG Labtech) at 490 nm directly correlates with the level of cytotoxicity. To minimize background noise, absorbance was also measured at 680nm and subtracted from the 490nm readings. Cells were cultured under standardized conditions and treated as detailed in the results section. The assay was conducted in accordance with the manufacturer's protocol. For infected samples all steps were performed in a class II biological safety cabinet.

3.9. ELISA

Enzyme-linked immunosorbent assay (ELISA) is an immunoassay which can detect different substances from the supernatant of a sample, in this case cytokines, such as IL-1β (94). The Human IL-1 beta/IL-1F2 DuoSet ELISA kit (R&D Systems #DY201) contains capture and detection antibodies, standards and enzyme-linked secondary antibodies. 96-well plates from NUNC were used for detection. Wash buffers were made with Dulbecco's phosphate buffered saline (PBS) (Sigma-Aldrich #D8537-500ML) + 0,05% Tween 20. Reagent diluent were made with high quality bovine serum albumin (BSA) (Sigma-Aldrich #A7030-50G). 2% BSA in PBS, 0,2 um sterile filtered. Substrate solution 1:1 mix of substrate A and substrate B (BioLegend #421101). 1M stop solution H_2SO_4 were added before measuring by the FLUOstar omega microplate reader (BMG Labtech) at 450nm and 540nm. The assay was conducted following the manufacturer's protocol, with the modification that all reagent volumes added to the 96-well plate were halved. The washing steps were performed after manufacturers protocol. Assay range for DuoSet IL-1β ELISA: 3.9 - 250 pg/mL. A standard curve was generated using Excel to determine the concentration of IL-1β in the samples.

3.10. Active Caspase-1 immunoblotting

To evaluate the activation of the inflammasome in WI-38 human fibroblasts, immunoblotting for active caspase-1 was conducted using a modified version of a protocol developed by Christopher Jakobs, Eva Bartok, Andrej Kubarenko, Franz Bauernfeind, and Veit Hornung (95). Cells were seeded in 12-well plates, and both supernatants and lysates were collected for analysis. Lysates were processed as described in Section 3.7 on Western blotting. For this modified version, 500 µl of supernatant were mixed with 500 µl of methanol and 125 µl of chloroform in an Eppendorf tube. After vigorous vortexing for 30 seconds and centrifugation at 13,000 x g for 5 minutes, three distinct layers were formed: an aqueous phase, a protein layer, and a chloroform phase. The aqueous layer was removed, while the protein and

chloroform layers were left undisturbed. An additional 500 µl of methanol was added, and the tube was vortexed vigorously. The disrupted protein layer formed small white flakes. The samples were then centrifuged at 13,000 x g for 5 minutes to form a pellet of the protein. The supernatant was carefully removed without disturbing the pellet, which was then dried in a SpeedVac centrifuge until completely dry.

The dried protein pellet was reconstituted in 40 µl of 1X LDS sample buffer, vortexed vigorously for 1 minute, and briefly centrifuged at 13,000 x g to collect the sample at the bottom of the tube. The samples were then heated at 70°C for 10 minutes, vortexed again for 1 minute, and spun down. Samples was loaded onto a NuPage® Bis-Tris gel (4-12% nitrocellulose, Invitrogen #NP0322BOX) and electrophoresed in 1X MES SDS running buffer (Invitrogen #NP0002) at 200V for approximately 1.5 hours. Protein standards, SeeBlue™, and Magic Mark™, were used as molecular weight markers.
After electrophoresis, the subsequent steps were performed further as described in Section 3.7 Western blot analysis.

3.11. Statistical analysis

Data were gathered from 1-4 independent experiments. For statistical analyses, GraphPad Prism version 10.2.0 was utilized. One-Way ANOVA followed by Tukey's Honest Significant Difference test was applied for comparisons among multiple groups. Differences between variables was considered significant when $p \leq 0.05$ (*).

4 Results

HEp-2

4.1 RSV replication kinetics in HEp-2 cells

HEp-2 cells are a widely used cell model for studying viral infections and to propagate RSV (96). To characterize RSV replication kinetics HEp-2 cells were infected with RSV at a multiplicity of infection (MOI) of 3, and the levels of RSV fusion protein (F_0 and F_1) were analyzed at 12-, 24-, 36-, 48-, 60-, and 72-hours post-infection. The levels of RSV fusion protein, F_0 and F_1 increased from 24 to 72 hours post-infection with RSV (Figure 6). In summary, this suggest that RSV can infect and replicate in HEp-2 cell, with highest levels of RSV fusion protein at 72h post-infection.

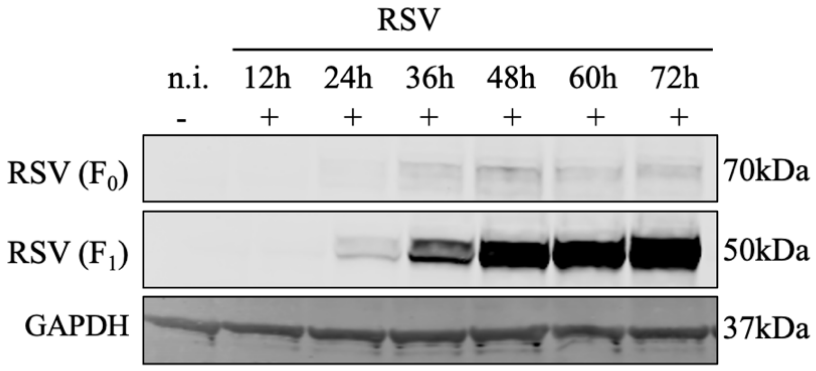

Figure 6. RSV replication kinetics in HEp-2 cells. Western blot showing the relative bands of RSV F1 and F0 fusion protein in RSV-infected HEp-2 cells at 12-, 24-, 36-, 48-, 60- and 72-hours, with a multiplicity of infection (MOI) of 3 or incubated with medium for 24 hours (n.i.). This data is compiled from one kinetic experiment. GAPDH was used as an endogenous control gene. The expected molecular weight of the detected bands is indicated in kilodaltons (kDa).

4.2 LDH release in RSV infected HEp-2 and WI-38 cells

Previous research has explored how RSV affects cell lines, pinpointing lactate dehydrogenase (LDH) as an indicator of cell damage (22). Synthetic molecules like poly(dA:dT) and poly(I:C), mimicking viral DNA and RNA, also trigger LDH release in cells (22, 65). Building on this, we aimed to study cell lysis, by LDH release, in response to RSV, p(dA:dT), and p(I:C) in HEp-2 and WI-38 cells.

Both cell lines were infected with RSV for 24- and 48 hours. Including two concentrations of p(dA:dT) and p(I:C) over a transfection period of 24 hours. A mock transfection control

(mock) serving as the control for comparing the effects of the synthetic analogs. In HEp-2 cells a significant increase in LDH release were observed at p(dA:dT) with a concentration of 2 µg/ml (Figure 7A). Additionally, in WI-38 cells, LDH release were significantly increased for both p(dA:dT) and p(I:C) at both tested concentrations (Figure 7B).

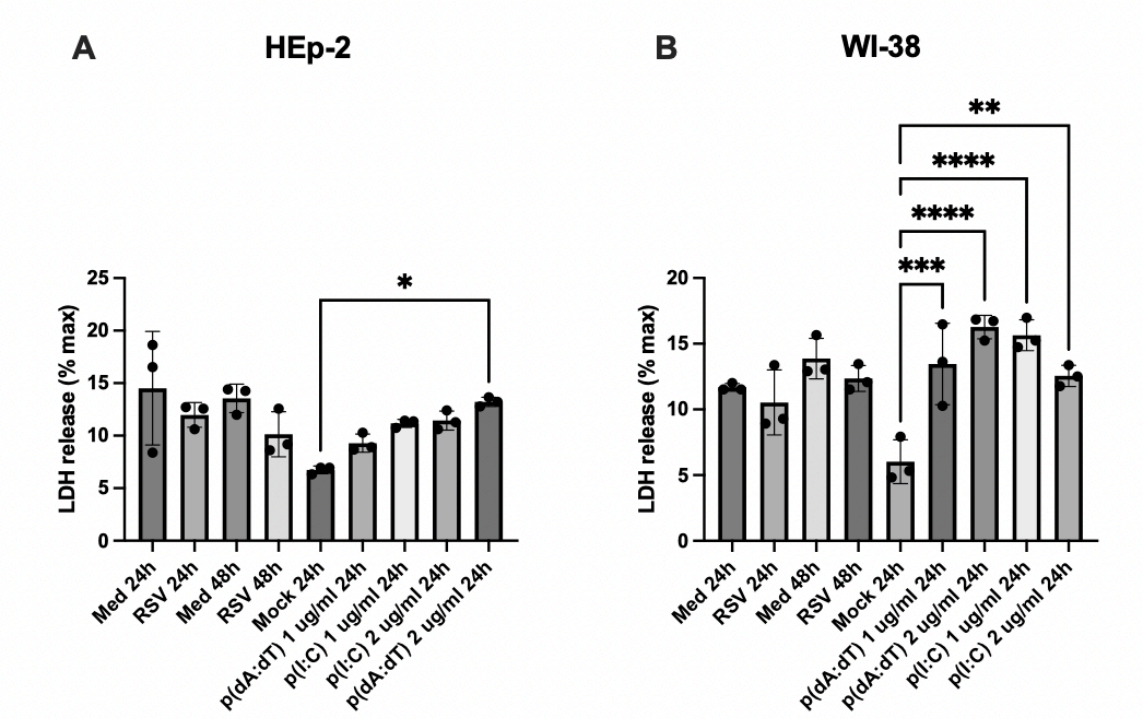

Figure 7. LDH release in HEp-2 and WI-38 cells. Both cell lines were treated with p(dA:dT) and p(I:C) at two concentrations (1 µg/ml and 2 µg/ml) transfected for 24h, mock serves as a control to the synthetic analogs p(dA:dT) and p(I:C). Cells were infected with RSV at a multiplicity of infection (MOI) of 3, assessed at both 24- and 48-hours post-treatment. Statistical analysis: Results presented are ± SEM of two experiments seeded in triplicates and analyzed by one-way ANOVA with Tukey's multiple comparisons test: ∗p < 0.05, **p< 0.01, ***p<0.001 and ∗∗∗∗p < 0.0001.

4.3 RSV infection induces TBK-1 phosphorylation in HEp-2 cells

NLRP3 protein level expression may vary with cell type (97). To examine if NLRP3 protein was expressed in HEp-2 cells, we infected HEp-2 cells with RSV and collected samples at various post-infection time points ranging from 12- to 72 hours. Western blot analysis was used to investigate NLRP3 protein levels across these time points post RSV-infection. Our results showed no detectable levels of NLRP3 protein in HEp-2 cells under any of the conditions tested (Supplementary S.3).

Given that NLRP3 induction is mediated through the NF-κB signaling pathway (98), we assessed whether RSV infection activates the NF-κB pathway by measuring levels of

phosphorylated NF-κB-P65 protein. No change in NF-κB-P65 protein expression was detected in RSV-infected HEp-2 cells (Figure 8). Concurrently, a time-dependent increase in TBK-1 phosphorylation, indicating that RSV triggers TBK1 activation, a kinase known to respond to RSV infection in HEp-2 cells (99).

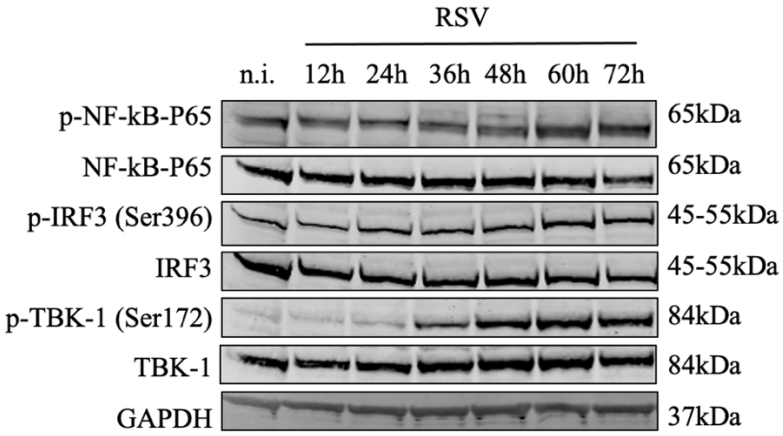

Figure 8. RSV induces TBK-1 phosphorylation in HEp-2 cells. The western blot shows RSV-infected HEp-2 cells at 12-, 24-, 36-, 48-, 60- and 72-hours, with a multiplicity of infection (MOI) of 3 or incubated with medium for 24h (n.i). Expression of p-NF-κB-P65, NF-κB-P65, p-IRF3 (Ser396), IRF3, p-TBK-1 (Ser172) and TBK-1 were assessed by western blot. GAPDH was used as an endogenous control. The presented data is compiled from one kinetic experiment. The expected molecular weights for the detected proteins are indicated in kilodaltons (kDa).

4.4 NLRP1 and NLRP3 expression in different cells

NLRP1 is predominantly observed in human keratinocytes and airway epithelial cells, whereas NLRP3 is commonly associated with monocytes, macrophages, and dendritic cells (63, 97). To assess the expression levels of NLRP1 and NLRP3 across various resting cells, we conducted RT-qPCR analysis on several cells known for their distinct expression patterns. The analyzed cells included A549 epithelial cells, Normal Human Dermal Fibroblasts (NHDF), Human Lung Fibroblasts (WI-38), Monocyte-Derived Macrophages (MDM), Peripheral Blood Mononuclear Cells (PBMCs), Neuroendocrine Cell Lines (NECs), and Human Epithelial type 2 (HEp-2) cells.

RT-qPCR analysis revealed detectable mRNA expression levels of NLRP1 and NLRP3 in PBMCs (Figure 9A and B), consistent with prior studies confirming their natural expression in these cells (63, 97). Additionally, NLRP3 mRNA levels were elevated in MDM cells (Figure 9B), while both NLRP1 and NLRP3 mRNA levels were increased in NECs relative to A549 cells (Figure 9A and B). In contrast, HEp-2 cells exhibited no expression of either

NLRP1 or NLRP3 mRNA, and WI-38 cells showed only slight expression of both genes (Figure 9A and B). Ct values from the RT-qPCR are available in Supplementary S.4.

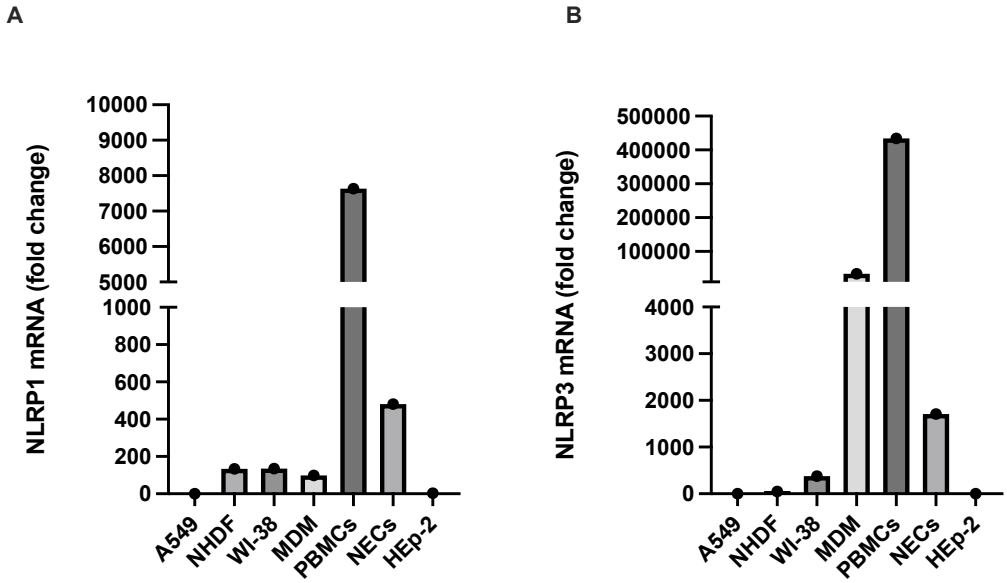

Figure 9. NLRP1 and NLRP3 expression in different cell lines. (A) NLRP1 and **(B)** NLRP3 mRNA expression was analyzed by RT-qPCR. Fold change values for each gene were normalized against GAPDH and calculated relative to A549 cells. A549 was chosen as the reference cell line because it is derived from human lung adenocarcinoma, known for its well-characterized phenotype and absence of NLRP1 and NLRP3 expression (22).

WI-38

Since HEp-2 cells did not express NLRP3 or NLRP1 mRNA, while WI-38 fibroblasts demonstrated moderate expression of both genes (Figure 9) along with increased LDH release in response to control cell death-ligands relative to HEp-2 cells (Figure 7), we chose to conduct further studies using WI-38 fibroblasts.

4.5 RSV replication kinetics in WI-38 cells

WI-38 cells have been historically underexplored in RSV research. To address if RSV can enter and replicate in WI-38 fibroblasts, cells were infected with RSV. Samples were collected over time from 12- to 72 hours post-infection. We observed a gradual increase of RSV fusion protein levels (F_0 and F_1) from 24- to 72 hours post-infection (Figure 10). This result indicates that RSV are able to enter and replicate in WI-38 cells, with highest levels of RSV fusion protein at 72h post-infection (Figure 10).

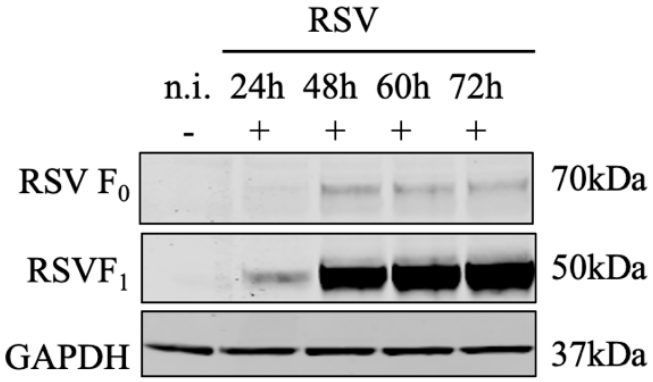

Figure 10. RSV replication kinetics in WI-38 cells. Western blot analysis of the protein levels of RSV fusion protein F_0 and F_1 in fibroblasts post-RSV infection, with a multiplicity of infection (MOI) of 3, at 24-, 48-, 60-, and 72-hours. The data is compiled from one kinetic experiment. GAPDH was used as an endogenous control. The expected molecular weights for the detected proteins are indicated in kilodaltons (kDa).

4.6 NLRP1 mRNA expression and protein levels in RSV-induced WI-38 fibroblasts

Given the understanding that NLRP1 can be activated by RNA viruses like RSV (100), we initially sought to explore if RSV-infection in WI-38 fibroblasts affected NRLP1 mRNA expression by RT-qPCR and protein levels by western blot analysis. WI-38 cells were infected with RSV, samples were collected over time from 24- to 72 hours post-infection. Synthetic analogs p(dA:dT) and p(I:C) were transfected at a concentration of 2.5 µg/ml for 24 hours.

RT-qPCR results does not show high levels of NLRP1 mRNA in WI-38 cells, but RSV infection suggest an increase in expression over time (Figure 11A). NLRP1 protein levels in RSV-infected fibroblasts was detected, both full length (160kDa) (Figure 11B). Macrophages and monocytes were added to this setup because they can express NLRP1 (Figure 11B). Monocytes are from two different donors (D1 and D2) and indicates a stronger NLRP1 expression in D1 (Figure 11B). Overall, based on mRNA and protein expression of NLRP1, it looks like RSV does not have any effect on NLRP1 levels in WI-38 cells.

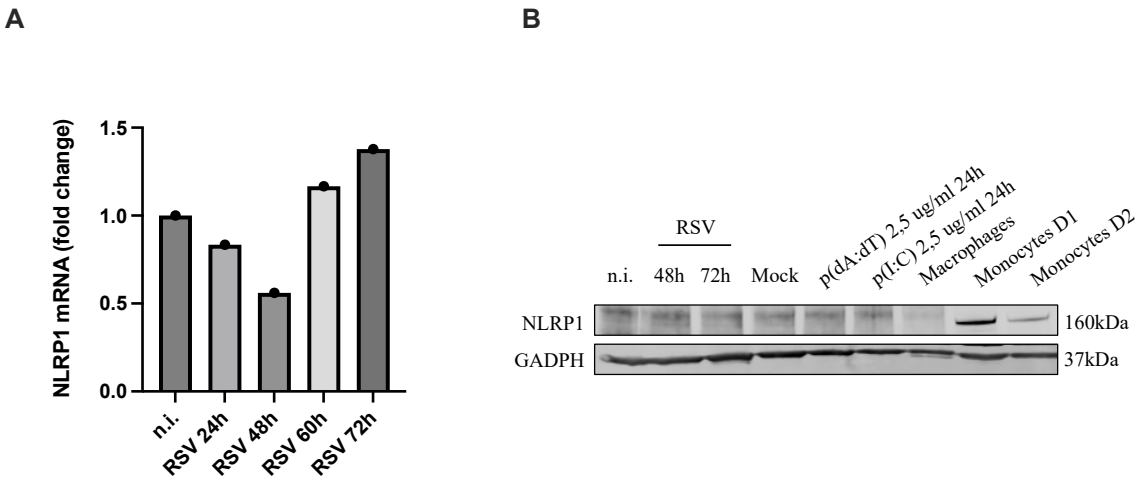

Figure 11. NLRP1 expression in WI-38 fibroblasts. RT-qPCR and western blot were used as techniques to identify any NLRP1. Both methods have treatments as non-infected cells (Med 24h/n.i.), RSV infected cells with a multiplicity of infection (MOI) of 3 for different timepoints. **(A)** RT-qPCR fold change in NLRP1 expression after treatments in WI-38 cells. Fold change values for each gene were normalized against GAPDH and calculated relative to non-infected cells (n.i.) **(B)** Western blot analysis illustrates NLRP1 protein levels in fibroblasts. Samples include transfection of p(dA:dT) and p(I:C) for 24h, mock serves as a control. Macrophages were added because they can express NLRP1. Two donors (D1 and D2) of monocytes were also added due to their expression of NLRP1. GAPDH was used as an endogenous control. One representative blot is shown from two biological replicates. The expected molecular weights for the detected proteins are indicated in kilodaltons (kDa).

4.7 LDH release increases with RSV infection time in WI-38 fibroblasts

As LDH release by RSV may occur during later stages of infection in different cell types (22), typically observed around the 72-hour mark, we aimed to evaluate whether RSV induces LDH release in WI-38 cells. LDH release is used as a marker of lytic cell death (22, 45).

WI-38 cells were infected with RSV for 48- and 72 hours. Hydrogen peroxide (H2O2) was used as a positive control for the LDH assay due to its well-known ability to induce oxidative stress in various cell types (101). Noting that poly(dA:dT) and poly(I:C) can induce LDH release in a variety of cell types (22), as observed in Figure 7, we treated WI-38 cells with these synthetic analogs to simulate viral infections of DNA and RNA, respectively. Additionally, we used ABT-737 as a control, because it induces mitochondrial death, leading to LDH release (102, 103).

LDH release of RSV induced fibroblasts shows a notable increase at 72-hours compared to 48 hpurs of infection (Figure 12A). We also observed that p(I:C) at 2.5 µg/ml resulted in significant LDH release at both 24- and 48 hours (Figure 12B). Furthermore, p(dA:dT) significantly increased LDH release with a concentration of 2.5 µg/ml, 48 hours after

transfection (Figure 12B). Lastly, ABT-737 triggered significant LDH release at a concentration of 10 uM after 24 hours, compared to vehicle (Figure 12B).

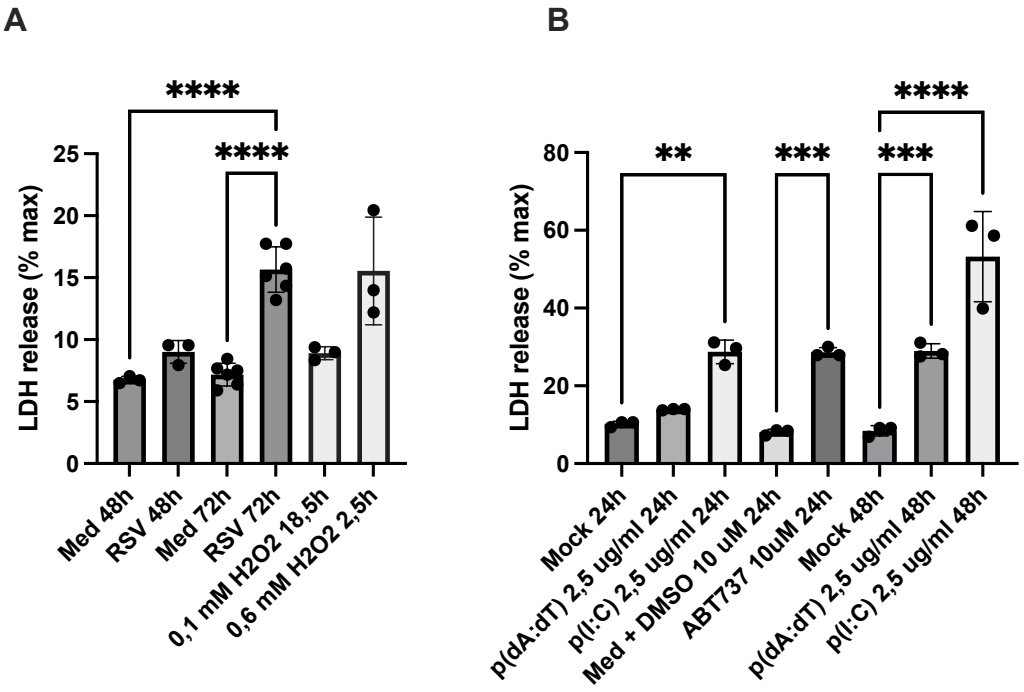

Figure 12. RSV induces LDH release. WI-38 cells were infected with RSV with a multiplicity of infection (MOI) of 3 for 48- and 72h. H2O2 serves as a control for LDH release with various concentration and time-points. p(dA:dT) and p(I:C), both at 2.5 µg/ml, administered for 24 and 48 hours. Mock serves as the control for the synthetic analogs. Vehicle control ("Med + DMSO 10uM") serving as a control for ABT737. **(A)** Shows LDH release in RSV-infected WI-38 cells for 48- and 72h. **(B)** Indicates LDH release of p(dA:dT), p(I:C) and ABT737 in WI-38 fibroblasts. Results presented are ± SEM of three independent experiments, seeded in triplicates and analyzed by one-way ANOVA with Tukey's multiple comparisons test: ∗p < 0.05, **p< 0.01, ***p<0.001 and ∗∗∗∗p < 0.0001.

4.8 RSV infection induces pro-IL-1β expression and IL-1β release in WI-38 fibroblasts

Activation of the NLRP1 or NLRP3 inflammasome leads to caspase-dependent cleavage of pro-IL-1β into active IL-1β, which can be released from cells (44). IL-1β release may be associated with cell death (22, 98, 104). To investigate whether RSV induces the expression of pro-IL-1β in WI-38 fibroblast cells, the cells were infected with RSV, and samples were collected at intervals from 24- to 72 hours post-infection. Synthetic analogs p(dA:dT) and p(I:C) were transfected for 24 hours. Additionally, we used ABT-737 as a control, because it induces mitochondrial death. The expression of pro-IL-1β protein were analyzed by western blot. Further, when pro-IL-1β is cleaved to form mature IL-1β, the presence of this cytokine in the supernatant can be quantitatively assessed using an immunoassay, such as an ELISA specifically designed for IL-1β.

We observed a gradual increase in cleaved IL-1β, indicated as pro-IL-1β protein levels, particularly between 48- to 72 hours post-infection (Figure 13A). This observation suggests that pro-IL-1β induction occurs in RSV-infected cells starting at 48 hours post-infection (Figure 13A). ELISA IL-1β analysis shows that RSV significantly increases IL-1β release in WI-38 fibroblasts after 72 hours (Figure 13B). The included synthetic analogs and ABT737, with mock- and DMSO controls, shows no IL-1β release (Figure 13B).

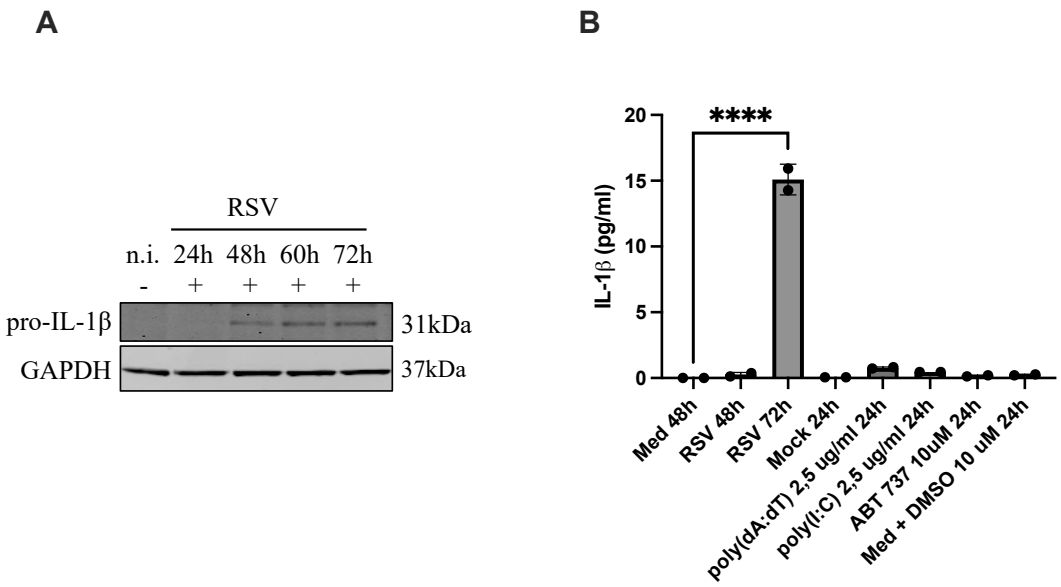

Figure 13. RSV induced pro-IL-1β expression and IL-1β release in WI-38 fibroblasts. (A) Western blot showing the relative bands of pro-IL-1β in RSV-infected WI-38 cells with a multiplicity of infection (MOI) of 3 at 48-, 60-, and 72 hours. This data is compiled from one kinetic experiment. GAPDH was used as an endogenous control gene. The expected molecular weight of the detected bands is indicated in kilodaltons (kDa). **(B)** ELISA IL-1β analysis of WI-38 cells treated with RSV with a multiplicity of infection (MOI) of 3 for 72h. p(dA:dT) and p(I:C) were transfected at a concentration for 24 hours, mock serves as a control. DMSO vehicle control for one concentration ABT737 ("Med + DMSO 10uM 24h"). Statistical analysis: Data presented are ± SEM of three experiments. The results were analyzed by one-way ANOVA with Tukey's multiple comparisons test: $*p < 0.05$, $**p< 0.01$, $***p<0.001$ and $****p < 0.0001$.

4.9 Caspase-1 detection in RSV-infected WI-38 fibroblasts

Formation of inflammasomes leads to the activation of caspase-1 which can trigger the maturation and release of cytokines and induce cell lysis (22). To investigate if we could detect active caspase-1 in RSV-infected WI-38 fibroblasts, we explored caspase-1 protein levels by western blot analysis. WI-38 cells were infected with RSV, and samples were collected at 48 and 72 hours post infection. Synthetic analogs p(dA:dT) and p(I:C) were transfected for 24 hours. Additionally, we used ABT-737 as a control.

The results indicated that RSV-infected cells at 48- and 72- hours shows an increase of pro--caspase-1 compared to non-infected cells (n.i.) (Figure 14). Pro-caspase-1 was also increased after treatment with p(dA:dT) and p(I:C) (Figure 14).

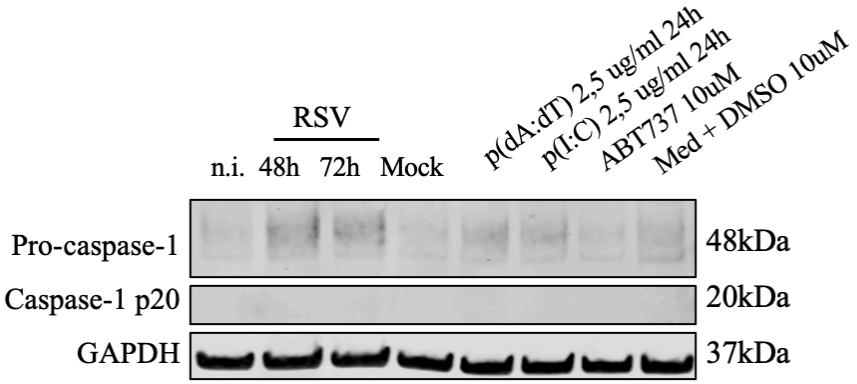

Figure 14. Caspase-1 detection in RSV-infected WI-38 fibroblasts. WI-38 fibroblasts were infected with RSV with a multiplicity of infection (MOI) of 3 for 48 and 72h. Synthetic analogs like p(dA:dT) and p(I:C) have a concentration at 2,5 μg/ml for 24h. Mock serves as a control for these synthetic analogs. DMSO vehicle control for one concentration ABT737 are indicated (Med + DMSO 10uM 24h). Western blot shows expression of pro-caspase-1 and caspase-1 cleaved p20 fragment. GAPDH was used as an endogenous control. One representative blot is shown from two biological replicates. The expected molecular weights for the detected proteins are indicated in kilodaltons (kDa).

To determine whether RSV triggers inflammasome activation through caspase-1 activation, we analyzed active caspase-1 in the supernatant of WI-38 cells by using western blot analysis, a method for caspase-1 as previously reported by Jakobs et al. (95). Unfortunately, the results showed that protein migration was likely distorted by fetal bovine serum (FBS) in medium and it was not possible to relate to molecular weight size and to detect active caspase-1 (Supplementary S.5).

4.10 Effect of NLRP1- and caspase inhibitors on RSV-induced IL-1β release and caspase-1 protein levels

To probe if inhibiting NLRP1 or caspase-1 affected RSV-mediated IL-1β release or caspase-1 levels, considering that NLRP1 may activate caspase-1, leading to IL-1β release (65, 105). QVD and VX765 are pan-caspase and caspase-1 inhibitor, respectively, and were included as controls. We investigated the impact of the newly developed NLRP1 inhibitor, ADS032 (106), on IL-1β release and caspase-1 protein levels in WI-38 fibroblasts following RSV infection.

Cells were pre-incubated with inhibitors before 72 hours of RSV infection. The effects of these inhibitors on RSV-induced IL-1β release were measured using ELISA.

The results shows that the inhibition of NRLP1, ADS032, at 20uM resulted in elevated levels of RSV-induced IL-1β release, whereas a strong reduction in RSV-induced IL-1β release was observed at 100 μM and 350 μM (Figure 15A). In contrast, the caspase-1 inhibitor, VX765, demonstrated a dose-dependent decrease on RSV-induced IL-1β release, with lower levels observed at higher concentrations (Figure 15A). This suggests that caspase-1 is involved in RSV-stimulated IL-1β release. The pan-caspase inhibitor QVD reduces RSV-induced IL-1β release (Figure 15A). Next, the effect of ADS032, VX765 and QVD on RSV levels was addressed by western blot analysis. NLRP1 inhibitor decreased the levels of RSV-induced RSV fusion protein levels, with increasing concentration of the inhibitor (Figure 15B). Caspase-1 and pan-caspase inhibitors did not affect RSV-induced RSV fusion protein levels, compared to the vehicle control (Figure 15B).

It has been suggested that caspase-1 levels is sufficient to induce inflammation (107). To investigate if the NLRP1 inhibitor affected caspase-1 levels in RSV-infected and p(dA:dT)-treated WI-38 fibroblasts, cells were pre incubated with NLRP1 inhibitor prior to infection with RSV for 72 hours and transfection of p(dA:dT) for 24h. The results show that we see an increase in pro-caspase-1 protein levels in RSV-infected cells (Figure 15C). RSV- and p(dAdT)-treated cells shows a decrease in pro-caspase-1 protein levels with increasing concentration of the NLRP1 inhibitor, compared to vehicle and mock control (Figure 15C). A slight increase is observed in cleaved caspase-1 p20 levels for all samples, except in RSV-infected cells with the highest concentration of NLRP1 inhibitor (Figure 15C).

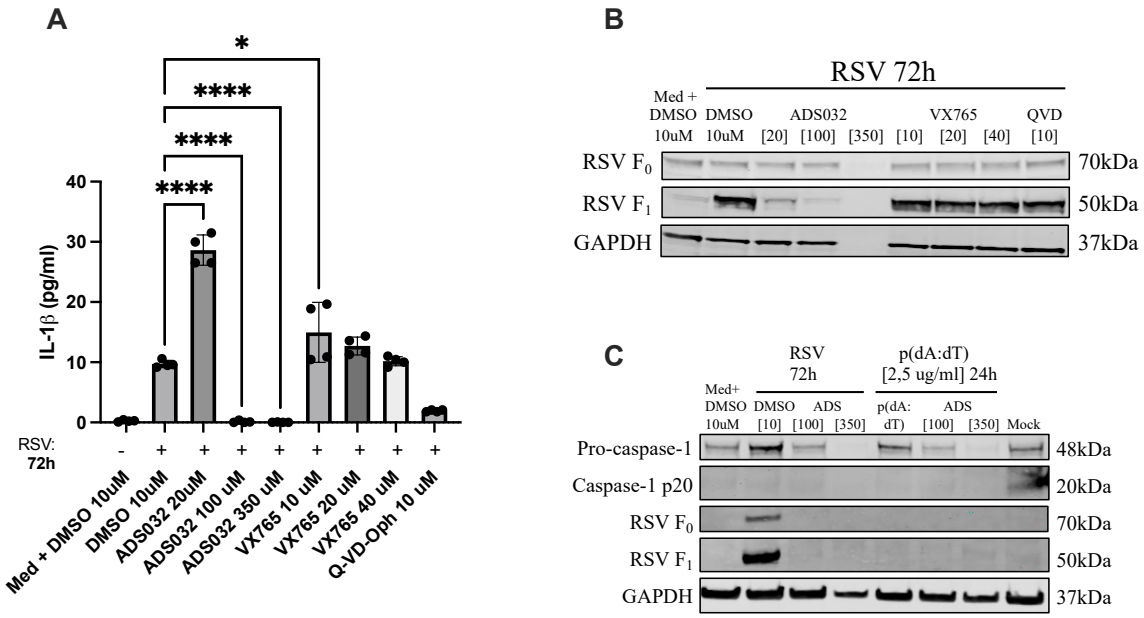

Figure 15. Effect of NLRP1- and caspase inhibitors on RSV-induced IL-1β release and caspase-1 levels. WI-38 cells were exposed to RSV multiplicity of infection (MOI) 3 with or without co-treatment of different inhibitors, including NLRP1 inhibitor (ADS032 at varying concentrations), a caspase-1 inhibitor (VX-765 at varying concentration), and a caspase inhibitor (Q-VD-OPh 10uM). Inhibitors were pre-incubated for 35 minutes prior to treatment with RSV for 72h or p(dA:dT) for 24h. **(A)** ELISA quantification of IL-1β concentration in pg/ml. Statistical analysis: Data presented are ± SEM of one independent experiments with two biological replicates and analyzed by one-way ANOVA with Tukey's multiple comparisons test: ∗p < 0.05, **p< 0.01, ***p<0.001 and ∗∗∗∗p < 0.0001. **(B)** Western blot shows expression of RSV fusion protein (F0 and F1). GAPDH was used as an endogenous control. The expected molecular weights for the detected proteins are indicated in kilodaltons (kDa). One representative blot is shown from two biological replicates. **(C)** Western blot shows expression of pro-caspase-1, caspase-1 cleaved p20 fragment, RSV fusion protein F_0 and F_1. GAPDH was used as an endogenous control. One representative blot is shown from two biological replicates. The expected molecular weights for the detected proteins are indicated in kilodaltons (kDa).

4.11 Effect of NLRP1-, caspase- and ValBoro Pro inhibitors on RSV induced IL-1β release

ValBoro Pro (VBP) has been shown to induce the release of the pro-inflammatory cytokine IL-1β in various cell lines (22). VBP inhibits the dipeptidyl peptidases DPP8, and DPP9 and can lead to activation of NLRP1 (22, 65). Hence, we addressed if VBP in fibroblasts affected IL-1β by ELISA. Additionally, we explored how inhibition of NLRP1 and caspase-1 impact RSV-induced NLRP1 protein levels by western blot analysis, given that NLRP1 can activate caspase-1 (65, 105).

WI-38 fibroblasts were pre-incubated with ADS032-, VX765-, QVD- and VBP inhibitors before being infected with RSV for 72 hours. The results interestingly shows that VBP increased RSV-induced IL-1β (Figure 16A), yet exhibited no effect when added alone, without RSV (Figure 16B). The ADS032 inhibitor demonstrated a dose-dependent reduction

in RSV induced NLRP1 protein levels (Figure 16C). At last, levels of the RSV fusion protein in cells exposed to RSV were reduced at the lowest concentration of the ADS032 inhibitor and were eliminated at the highest concentration (Figure 16C), consistent with previous observations.

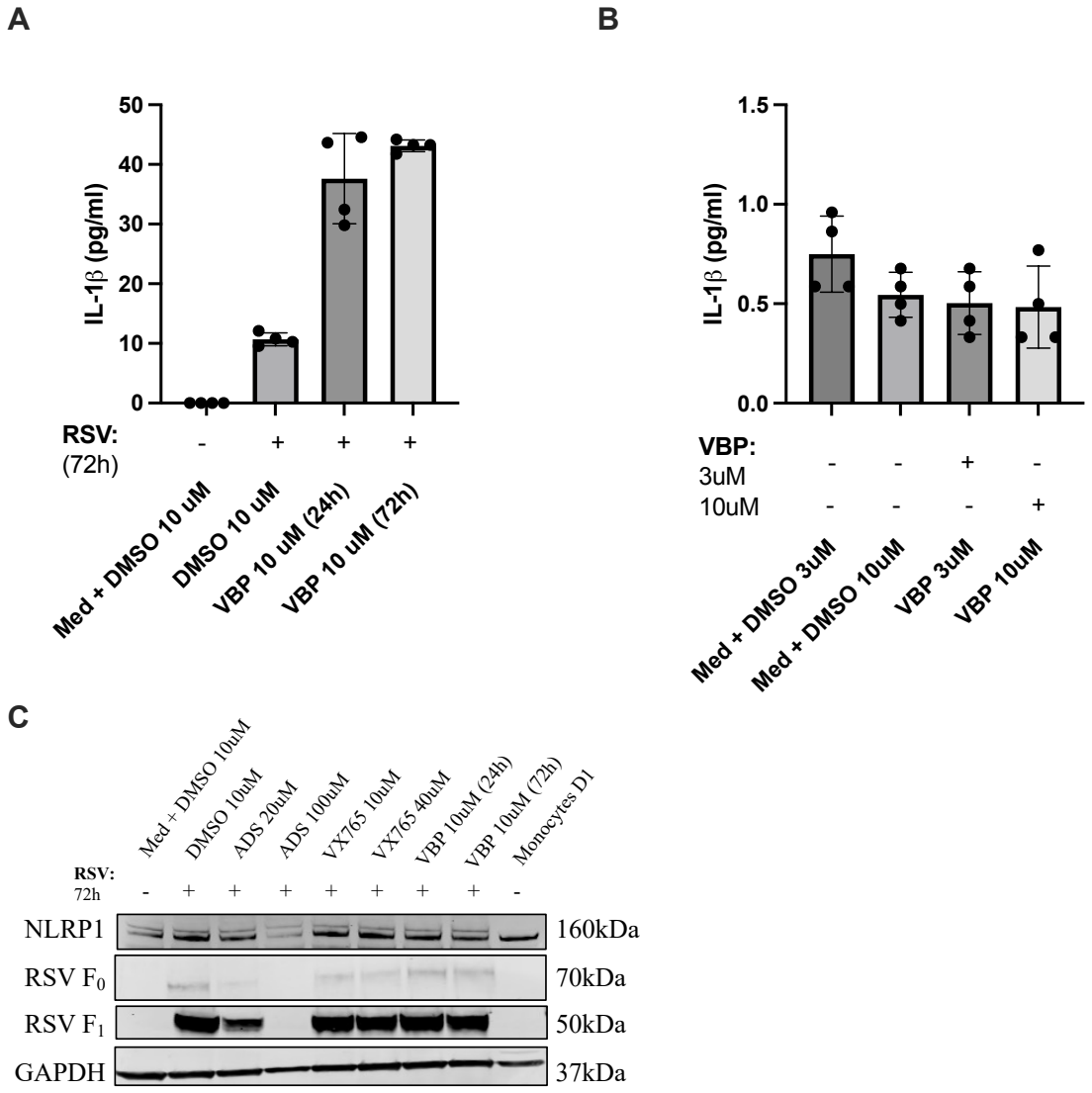

Figure 16. Effect of NLRP1-, caspase- and ValBoro Pro inhibitors on RSV induced NLRP1 protein levels and ValBoro Pro inhibitors on RSV induced IL-1β release. WI-38 fibroblasts were pre-incubated with NLRP1 inhibitor ADS032, caspase-1 inhibitor VX765 and ValBoro Pro (VBP) inhibitors for 35 minutes. Data are presented as one experiment with two biological replicates. **(A)** WI-38 fibroblasts were infected with RSV at a multiplicity of infection (MOI) of 3 for 72 hours, and VBP inhibitor was added for 24- and 72 hours. ELISA quantification of IL-1β concentration in pg/ml. Data are presented as one experiment with two biological replicates. **(B)** Treatments included controls and various concentrations of VPB. No significant results were found as the detected IL-1β release are below assay range. **(C)** WI-38 fibroblasts were infected with RSV at a multiplicity of infection (MOI) of 3 for 72 hours. ELISA quantification of IL-1β concentration in pg/ml. Statistical analysis of IL-1β ELISA: Data presented are ± SEM of two independent experiments with two biological replicates and analyzed by one-way ANOVA with Tukey's multiple comparisons test: $*p < 0.05$, $**p< 0.01$, $***p<0.001$ and $****p < 0.0001$.

4.12 RSV infection induces DNA damage and cGAS expression in WI-38 fibroblasts

γH2AX is a DNA damage signal associated with double strand breaks (DSBs) and cell death (108, 109). P(dA:dT) and p(I:C) were used as controls because they have been shown to induce γH2AX in keratinocytes (65). ABT-737 induces mitochondrial-dependent apoptosis (103). To examine if RSV induces DSBs in fibroblasts, WI-38 cells were infected with RSV, samples were collected at 48- and 72-hours post-infection. The results indicated an increase in γH2AX protein levels in RSV-infected samples, with more pronounced expression observed at 72 hours post-infection compared to 48 hours (Figure 17). Synthetic analogs p(dA:dT) and p(I:C), as well as ABT737, each show a strongly increase in γH2AX protein levels in WI-38 fibroblasts (Figure 17).

Prior research has shown that DNA damage can activate the cGAS-STING pathway (80). Recent study indicate that the activation of the cGAS-STING pathway can lead to the activation of NLRP3 inflammasomes, which are crucial for the immune response in cells like monocytes (110). In our study, we observed an increase in cGAS protein levels in RSV-infected cells (Figure 17). While no significant changes in phosphorylated STING (p-STING) levels in RSV-infected WI-38 cells, STING was present in all samples with a moderate increase following RSV treatment (Figure 17). Phosphorylated TBK-1 was detected in RSV-infected cells at 48- and 72 hours post-infection (Figure 17). Of the controls, p(dA:dT) strongly induced cGAS, p-STING, and phosphorylated TBK-1 (Figure 17).

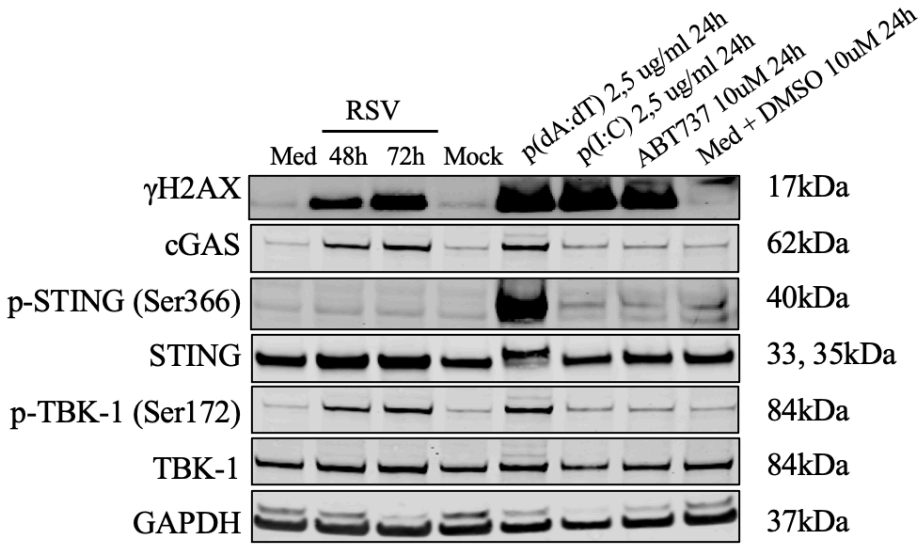

Figure 17. RSV induces DNA damage, cGAS and phosphorylated TBK-1 expression. WI-38 fibroblasts were infected with RSV with a multiplicity of infection (MOI) of 3 for 48 and 72h. Synthetic analogs like p(dA:dT) and p(I:C) have a concentration at 2,5 µg/ml for 24h. Mock serves as a control for these synthetic analogs. DMSO vehicle control for one concentration ABT737 are indicated (Med + DMSO 10uM 24h). Western blot shows expression of γH2AX, cGAS, p-STING (Ser366), STING, p-TBK-1 (Ser172) and TBK-1. GAPDH was used as an endogenous control. The expected molecular weights for the detected proteins are indicated in kilodaltons (kDa). One representative blot is shown from two biological replicates.

4.13 Effect of STING- and pan-caspase inhibitors on RSV, p(dA:dT) and ABT737 induced DNA damage and IL-1β release in WI-38 fibroblasts

DNA damage has been found to associate with IL-1β release (65, 111), and DNA damage may induce STING-dependent inflammation (112, 113). Caspases are central to the processing of pro-IL-1β into IL-1β, within the inflammasome (75). Due to the reported interactions between inflammation and DNA damage we next evaluated if the STING- or pan-caspase inhibitors affected RSV-stimulated γH2AX protein levels. WI-38 cells were preincubated with STING inhibitor C171. The pan-caspase inhibitor QVD was included as a control, as IL-1β release is caspase dependent.

The result shows that pan-caspase inhibitor reduced RSV-induced γH2AX (Figure 18A). While there was no significant difference in RSV-induced STING protein levels for none of the inhibitors, compared to the vehicle control (Figure 18 A, D and E). Further, whether the STING or pan-caspase inhibitor affected RSV-induced IRF3 protein levels compared to the vehicle control (Figure 18A, F and G). At last, we wanted to address if STING- and pan-caspase inhibitors modulates RSV induced IL-1β by ELISA. The results shows that pan-caspase inhibitor reduced RSV-induced IL-1β release, indicating that caspases contribute to

IL-1β secretion, while the STING inhibitor did not affect IL-1β release under the tested concentrations and exposure durations (Figure 18B).

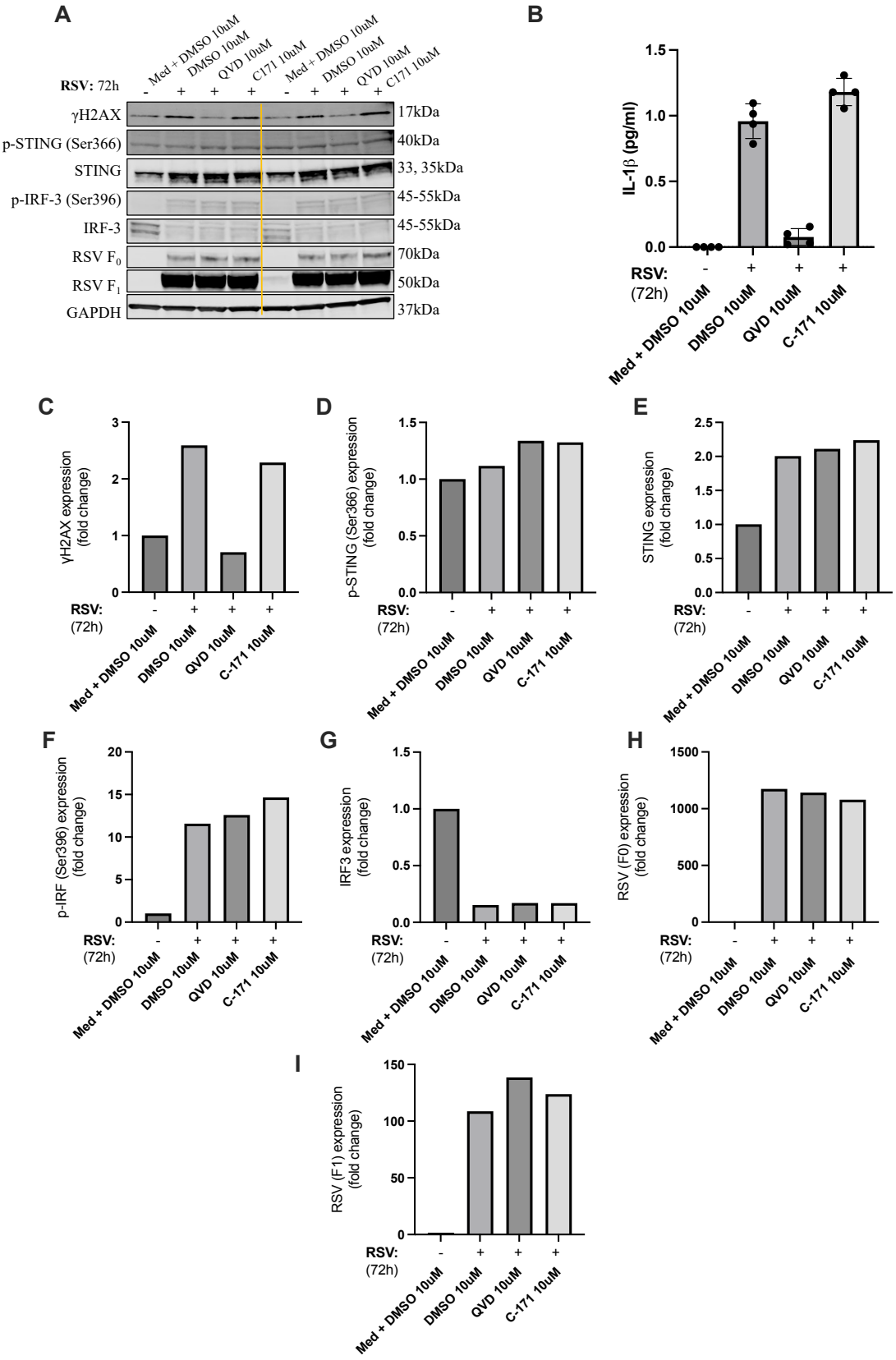

Figure 18. Effect of STING- and pan-caspase inhibitors on RSV induced DNA damage and IL-1β release. WI-38 cells were pre-incubated with STING-inhibitor C171 and pan-caspase-inhibitor Q-VD-OPH (QVD) with

a concentration of 10uM for 35 minutes prior to RSV infection with a multiplicity of infection (MOI) of 3 for 72h. Vehicle DMSO control for the inhibitors is indicated (Med + DMSO 10uM). **(A)** The western blot was performed using a single gel that contains biological duplicates. Western blot shows expression of γH2AX, p-STING (Ser 366), STING, p-IRF3 (Ser 172), IRF3, and RSV F_0 and F_1. GAPDH was used as an endogenous control. The expected molecular weights for the detected proteins are indicated in kilodaltons (kDa). **(C)** γH2AX **(D)** p-STING (Ser 366) **(E)** STING **(F)** p-IRF3 (Ser 172), **(G)** IRF3 **(H)** RSV F_0 and **(I)** RSV F_1 protein levels were quantified and normalized against GAPDH. The protein levels are presented as fold change relative to non-infected cells (Med + DMSO 10uM). **(B)** ELISA IL-1β analysis of various treatments indicating the effects of QVD and C171. Statistical analysis of IL-1β ELISA: Data presented are ± SEM of one independent experiments with two biological replicates. Due to the low release of IL-1β, no significant results were found.

To examine if STING- and pan caspase inhibitors affected p(dA:dT) and ABT737 induced γH2AX and IL-1β release, WI-38 cells were pre-incubated with inhibitors before p(dA:dT)-transfection and addition of ABT737, for 24h. The results shows that the pan-caspase inhibitor decreased p(dA:dT) and ABT737 induced γH2AX protein levels, as seen for RSV, without effect on phosphorylated STING and -IRF3 protein levels (Figure 19A). Given that STING has been implicated in the DNA-driven inflammasome activation and IL-1β release (PNAS Zhou), we investigated whether STING and a pan-caspase inhibitor induced IL-1β release by p(dA:dT) and ABT737. Results shows that pan-caspase inhibitor decreased p(dA:dT) induced IL-1β (Figure 19B), as seen for RSV. Further, ABT737 did not induce IL-1β (Figure 19B), also observed in figure 13B.

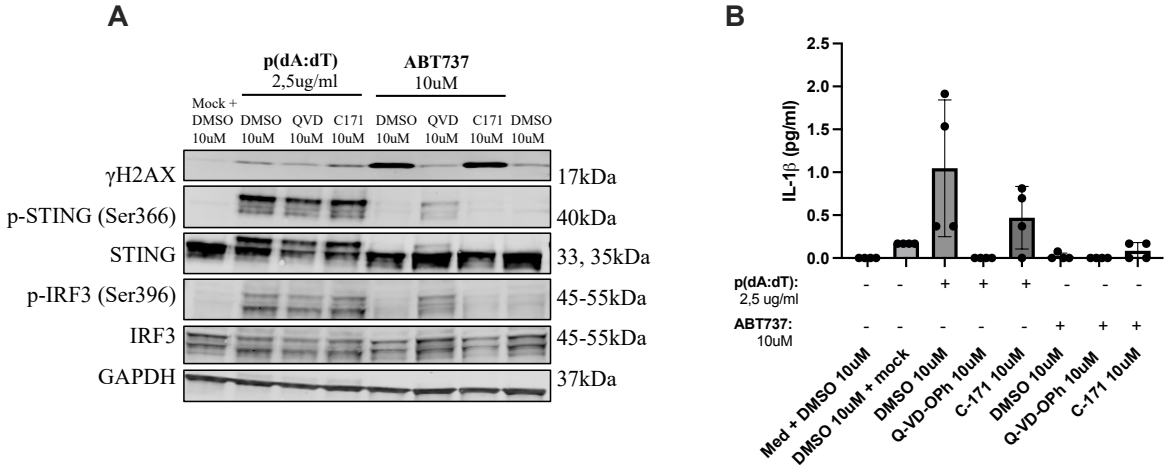

Figure 19. Effect of STING- and pan-caspase-inhibitors on poly(dA:dT) and ABT737 induced DNA damage and IL-1β release in WI-38 fibroblasts. Cells were pre-incubated with STING-inhibitor C171 and pan-caspase-inhibitor Q-VD-OPH (QVD) for 35 minutes, prior to p(dA:dT) transfection and addition of ABT737 for 24h. Mock serves as a control to p(dA:dT) and vehicle DMSO control for the inhibitors is indicated (Med + DMSO 10uM). **(A)** Western blot shows expression of γH2AX, p-STING (Ser 366), STING, p-IRF3 (Ser 172) and IRF3. GAPDH was used as an endogenous control. One representative blot is shown from two biological replicates. The expected molecular weights for the detected proteins are indicated in kilodaltons (kDa). **(B)** ELISA IL-1β analysis of various treatments indicating the effects of QVD and C171 inhibitors on p(dA:dT) and ABT737. Statistical analysis of IL-1β ELISA: Data presented are ± SEM of one independent experiments with two biological replicates. Due to the low release of IL-1β, no significant results were found.

4.14 Effect of ATM-, ATR- and PARP inhibitors on RSV-induced DNA damage

The kinases ATM, ATR and PARP are implicated in the cellular response to DNA damage (114-116). As we found that RSV stimulated γH2AX, we next addressed if inhibitors of ATM, ATR and PARP affected γH2AX in RSV-infected fibroblasts. WI-38 cells were pre-incubated with ATM-, ATR- and PARP inhibitors (ATMi, ATRi and PARPi) followed by infection with RSV.

The result indicated that the ATM inhibitor increase RSV-induced γH2AX at the lowest concentration, compared to the higher concentration (Figure 20A and B). Further, the ATR inhibitor increased RSV-induced γH2AX at the highest concentration (Figure 20A and B). Interestingly, the ATM inhibitor reduced RSV-induced RSV fusion protein levels at the highest concentration (Figure 20A). At last, the ATM inhibitor increased RSV-induced p-IRF3 protein levels (Figure 20A and C).

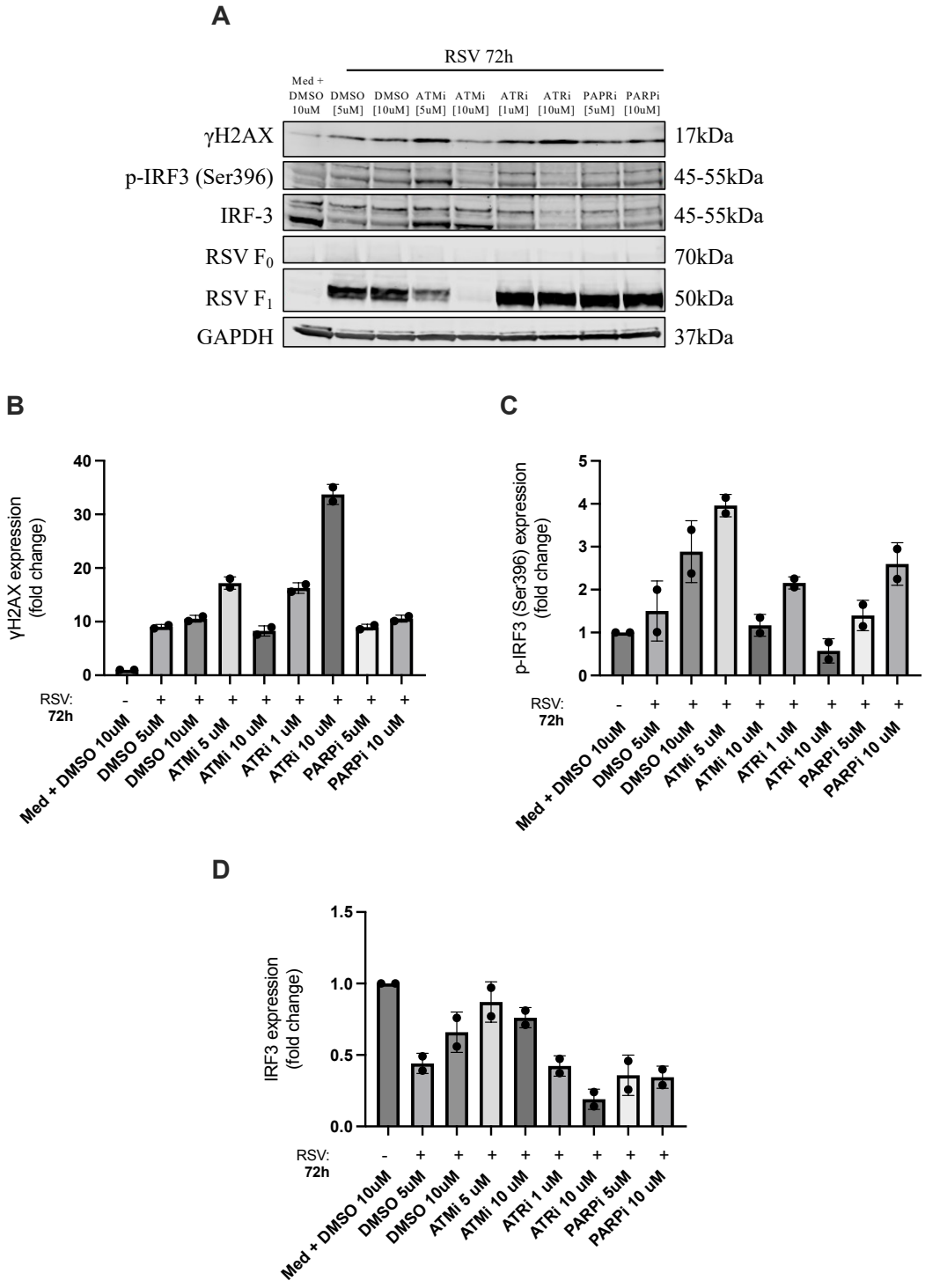

Figure 20. Effect of inhibitors of DNA damage signal transducers on RSV-induced DNA damage. WI-38 cells were pre-incubated with inhibitors for 35 minutes, and then infected with RSV multiplicity of infection (MOI) 3 for 72 h. Western blot shows expression of γH2AX, RSV F_0 and F_1, p-IRF3 (Ser 172), IRF3, p-STING (Ser 366), STING. GAPDH was used as an endogenous control. The expected molecular weights for the detected proteins are indicated in kilodaltons (kDa). One representative blot is shown from two biological replicates. **(B)** γH2AX **(C)** p-IRF3 (Ser 172) and **(D)** IRF3 protein levels were quantified. Protein levels were quantified and normalized against GAPDH. The protein levels are presented as fold change relative to non-infected cells (Med + DMSO 10uM). Data presented are the mean ± SD from two biological replicates.

4.15 Effect of ATM-, ATR- and PARP inhibitors on RSV-induced IL-1β release in WI-38 fibroblasts

To further explore the impact of the ATM, ATR and PARP inhibitors on RSV-induced responses in WI-38 cells, we measured IL-1β secretion using ELISA. WI-38 fibroblasts were treated with three different enzyme inhibitors with several concentrations and infected with RSV for 72 hours. Due to the observation of a high number of dead cells in the wells treated with ATM inhibitor and RSV prior to lysis, we anticipated a significant increase in IL-1β release, which was indeed confirmed by ELISA (Figure 21A and B). This outcome suggests a dose-dependent response associated with the ATM inhibitor on RSV-induced IL-1β. Furthermore, the highest concentration of the ATR inhibitor showed the highest increase of RSV-induced IL-1β release (Figure 21A and B). Finally, the PARP inhibitor led to an increase in RSV-induced IL-1β at the highest concentration (Figure 21A). However, the difference between the two concentrations of PARP inhibitor was less pronounced in RSV induced IL-1β (Figure 21B).

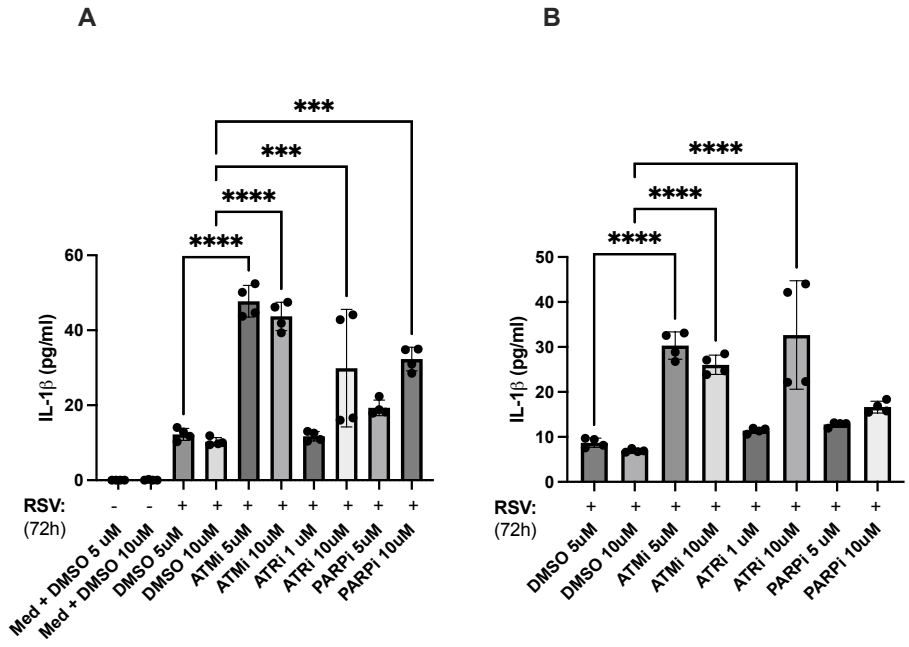

Figure 21. Impact of enzyme inhibitors on IL-1β release in RSV-infected WI-38 cells. ELISA IL-1β **(A)** and **(B)** display the result of two independent biological replicates investigating IL-1β release following RSV infection with a multiplicity of infection (MOI) of 3 for 72 hours, in the presence of three enzyme inhibitors at two different concentrations. Inhibitors were pre-incubated for 35 minutes prior to RSV infection. In figure 21B, medium samples were not analyzed as they have consistently shown no IL-1β release in previous experiments. Statistical analysis: Data presented are ± SEM of two independent experiments with two biological replicates each and analyzed by one-way ANOVA with Tukey's multiple comparisons test: ∗p < 0.05, **p< 0.01, ***p<0.001 and ∗∗∗∗p < 0.0001.

5 Discussion

Cell death mechanisms and components in relation to RSV infection of WI-38 fibroblasts plays a central role of mediating the immune response. In this thesis we explored that RSV induces lytic cell death along with IL-1β release. As well as how NLRP1- and caspase inhibitors gives effects on IL-1β release and γH2AX protein levels in RSV-induced WI-38 fibroblasts. In this thesis some aspects related to cell death and IL-1β release in RSV-infected lung fibroblasts were explored.

5.1 RSV induced LDH- and IL-1β release, and DNA damage in WI-38 fibroblasts

RSV infection led to a significant increase in LDH release in WI-38 lung fibroblasts, suggesting lytic cell death (Figure 12A). The degree of LDH release varied significantly when compared to HEp-2 cells, underscoring the cell-type dependent nature of RSV-induced LDH-release (22). Such variability underscores the complexities in defining a universal threshold for LDH release that conclusively indicates cell death, as cytotoxicity levels are profoundly influenced by factors such as the cell types sensitivity to RSV and the experimental conditions applied (22). This observation aligns with existing literature that identifies RSV as a trigger for cell death pathways such as pyroptosis and necroptosis in different cellular contexts (22, 45).

Following RSV infection, there was a notable increase in IL-1β release in WI-38 cells (Figure 13). This suggests that the inflammasome pathway, which is critical for the maturation and secretion of IL-1β, is activated in response to viral infection (98). Notably, the data aligns with the hypothesis that RSV infection can promote an inflammatory response through the NLRP3 inflammasome pathway, leading to the secretion of pro-inflammatory cytokines, a mechanism that has been observed in similar pulmonary infections (98, 117, 118).

Additionally, our studies revealed an increase in γH2AX protein levels, a marker for DNA double-strand breaks, indicating genetic damage due to RSV infection (85). This increase is likely driven by oxidative stress induced by RSV, further evidenced by previous studies where they have found elevated ROS production during virus infections (54). These reactive oxygen species are capable of inducing cellular damage, including DNA double-strand breaks as marked by γH2AX, suggesting that the impact of RSV extends beyond compromising cell viability to inducing substantial genetic damage (54, 85). The pronounced upregulation of

γH2AX post-RSV exposure emphasizes the potential of RSV to cause genotoxic stress in WI-38 fibroblasts. This genotoxic stress could have profound implications for cellular function and viability, potentially leading to cell cycle arrest, apoptosis, or other forms of cell death, thereby contributing to the overall pathogenicity of the virus (109).

Future research should focus on defining cell-type specific responses to RSV, particularly examining LDH release as an indicator of cell death across different cell lines. Additionally, understanding the dynamics of inflammasome activation in various cellular environments is crucial for comprehending the pathogenic mechanisms of RSV and for the development of targeted therapies.

5.2 Impact of RSV on NLRP1 and NLRP3 inflammasome activation in WI-38 fibroblasts

Further we investigated the impact of RSV on different inflammasomes and their activation. Our findings indicate a moderate expression of NLRP1 mRNA in WI-38 cells (Figure 9), which contrasts with the higher expression levels reported in primary human fibroblasts and specific epithelial cells (22, 63, 65). This suggests that RSV can modulate NLRP1 mRNA expression and protein stability, a finding that underscores the need for further exploration of inflammasome involvement in RSV-induced IL-1β release and cell death. Given the complexity of inflammasome pathways, the specific triggers and regulatory mechanisms influenced by RSV warrant further investigation, potentially revealing novel aspects of virus-host cell interaction dynamics.

Interestingly, studies by Poeck et al. (119), demonstrate that RIG-I and ASC can form an NLRP3-independent inflammasome, suggesting a mechanism where RIG-I may directly facilitate ASC-caspase activation, contributing to IL-1β cleavage independently of traditional inflammasome pathways (119). This pathway could represent an alternative or supplementary inflammatory response to RSV infection, which may be particularly relevant in cells where NLRP3 is not the predominant inflammasome. Consistent with these findings, our observations indicate that the application of QVD, a pan-caspase inhibitor, substantially reduced RSV-induced IL-1β release without altering RSV fusion protein levels, underscoring the critical role of caspases in mediating this inflammatory response (Figure 15A and B). Such findings suggest that caspase activation might be a critical step in the inflammasome

signaling cascade triggered by RSV, further emphasizing the potential therapeutic value of caspase inhibitors in managing RSV-induced inflammation.

While inflammasomes such as NLRP1 are important for IL-1β production (63), our data suggest that their presence alone is insufficient to initiate IL-1β secretion in WI-38 cells (Figure 16B). Instead, the enhancement of IL-1β release by RSV implies that viral factors, possibly in conjunction with signals from inflammasome activators like VBP are necessary to fully activate this cytokine's release (Figure 16A). These results are supported by studies which demonstrated that the activation of NLRP1 and NLRP3 inflammasomes in Alzheimer's disease is associated with increased cytokine production, suggesting that inflammasome components require additional pathogenic or cellular stress signals to effectively mobilize cytokine processing and secretion (120). Additionally, another study highlights the role of the NLRP3 inflammasome in lung inflammation induced by pathogenic particles and fibers, reinforcing the idea that environmental and pathogenic factors significantly influence inflammasome activity and cytokine release (121).

Looking forward, it is crucial to further explore the differential expression and function of NLRP1 in various cell types, especially in the context of how RSV modifies inflammasome activity. Additionally, the role of non-canonical pathways, such as the RIG-I and ASC complex, in RSV-induced IL-1β release should be investigated. These studies could provide deeper insights into the inflammatory pathways activated by RSV and help identify potential targets for therapeutic intervention. Understanding these mechanisms in greater detail will be key to developing more effective treatments for RSV and similar respiratory viruses that exploit similar immunological pathways. Future investigations should also consider the temporal dynamics of inflammasome activation in response to RSV, potentially revealing insights into the progression of immune responses during infection. This could involve longitudinal studies tracking inflammasome component levels and activity from initial infection through to recovery or progression to more severe disease states.

5.3 The effect of ValBoro Pro inhibitor on RSV-induced WI-38 fibroblasts

ValBoro Pro (also known as Talabostat or PT-100) has been recognized for its ability to inhibit dipeptidyl peptidase (DPP) activity, which indirectly affects several immune signaling pathways (65). Research have shown that VBP enhances immune responses against tumor

cells by increasing the levels of cytokines and chemokines, including IL-1β, particularly in the context of cancer therapy (122). This prior understanding aligns with our findings, suggesting that VBP's role in immune modulation extends to viral infections, enhancing the host's inflammatory response when combined with viral insults.

In our experiments, VBP, a known activator of the NLRP1 inflammasome, did not independently trigger IL-1β secretion in WI-38 fibroblasts (Figure 16B). However, pre-incubation of these cells with VBP followed by RSV infection resulted in a significant increase in IL-1β release (Figure 16A). This observation underscores that while VBP can prime the NLRP1 inflammasome, the presence of RSV is crucial for the actual cytokine release, suggesting a synergistic interaction between inflammasome priming and viral infection-induced signals. Western blot analysis confirmed the upregulation of pro-IL-1β in response to RSV infection (Figure 13A). This implies that the mechanism underlying enhanced cytokine release may involve the co-activation of NLRP1 by RSV-induced pro-inflammatory signals, rather than by VBP alone.

Our results are supported by studies indicating that components like RIG-I, along with MAVS and CARD9, play critical roles in IL-1β production during viral infections, such as with Vesicular stomatitis virus, by engaging non-canonical inflammasome pathways (119). This propose that in the context of RSV infection, IL-1β release is likely mediated by a complex interaction between NLRP1 activation and the virus-mediated induction of pro-IL-1β, highlighting a potential multi-modal regulation of inflammatory responses in viral infections. Our results points to a nuanced role of NLRP1 in viral immunology, where inflammasome activators like VBP alone may not suffice to trigger robust inflammatory responses without concurrent viral or cellular stress signals. Identifying the precise interplay between viral components and NLRP1 activation could unveil new therapeutic targets to control excessive inflammation during viral infections, focusing on modulating inflammasome activity in sync with viral dynamics.

Future studies should delve into the specific mechanisms by which RSV and NLRP1 activators like VBP synergize to enhance IL-1β release. Investigating how RSV modifies inflammasome pathways and interacts with other immune signaling processes will be crucial for developing targeted interventions aimed at mitigating viral-induced inflammation.

5.4 Impact of STING- and caspase inhibitors on RSV-induced DNA damage and IL-1β release in WI-38 fibroblasts

First, the observed increase in cGAS protein levels, along with a moderate increase in STING phosphorylation in RSV-induced WI-38 fibroblasts (Figure 17), suggests an activation of the cGAS-STING pathway, a critical sensor of cytosolic DNA and mediator of innate immune response (79-81). The activation of cGAS-STING pathway not only underscores an essential antiviral response but also highlights potential therapeutic targets that could help enhance antiviral defenses while minimizing tissue damage and inflammatory responses.

The effects of the STING inhibitor, C171, were explored to ascertain its role in RSV-induced cellular responses. Contrary to its effects in other cellular models, C171 did not significantly affect RSV-induced changes in WI-38 cells. This aligns with findings from Zhou et al. (65), where STING does not contribute to p(dA:dT)-induced IL-1β release in keratinocytes, suggesting cell-type specific differences in the pathway engagement. Our analysis revealed a marked phosphorylation of STING following p(dA:dT) treatment compared to RSV-infected or p(I:C) transfected cells (Figure 17). It remains to address if p(dA:dT)-mediated IL-1β or STING phosphorylation in WI-38 cells are related to NRLP1 function.

Further analysis using the NLRP1 inhibitor, ADS032, demonstrated a decrease in RSV-induced fusion protein levels, suggesting that RSV may exploit NLRP1-driven processes for effective replication (Figure 15B and C, and Figure 16C). Contrastingly, caspase inhibitors, QVD and VX765, variably affected RSV-induced IL-1β release, with QVD significantly inhibiting it, indicating a crucial role of caspases in mediating RSV-induced inflammatory responses (Figure 18B). Interestingly, ADS032, primarily an NLRP1 inhibitor which may also affect NLRP3 at higher doses, showed distinct influences on RSV-induced IL-1β dynamics (Figure 15A), likely mediated through NLRP1 or unintended targets as NLRP3 protein levels was not detectable in WI-38 cells (Supplementary S.3).

Additionally, our study links the caspase pathway, particularly caspase-3, to RSV-triggered outcomes in WI-38 cells. The pan-caspase inhibitor QVD, which targets caspase-3 among others, reduced both IL-1β release and indicators of lytic cell death, underscoring a potential pathway via which RSV induces cellular effects. This suggests that caspase-3, rather than caspase-1, may play a more critical role in the mediation of RSV-induced cellular responses in WI-38 cells. The detection of pro-caspase-1 (Figure 14) supports this theory, although the

specific activation fragments of caspase-1 were not detectable, possibly due to technical challenges associated with assay conditions. These findings suggest a complex interplay between viral infection, inflammasome activation, and caspase pathways in determining cellular outcomes to RSV exposure. While STING does not seem to play a significant role in RSV responses in WI-38 cells, the roles of NLRP1 and caspases are important for understanding and possibly reducing the harmful effects of RSV.

Future studies should aim to further dissect these inflammasome- and caspase pathways, possibly employing NLRP1-specific modulation techniques like gene knockdown or activation via VBP, to clarify the interplay between viral infection, inflammasome activation, and caspase pathways in RSV responses. Further exploration of the role of STING, alongside NLRP1 and caspases, will be crucial for developing strategies to mitigate the harmful effects of RSV by modulating these pathways.

5.5 ATM inhibitor decrease the expression of RSV-induced RSV fusion protein levels and gave high IL-1β release

Our study investigated the role of ATM, a critical kinase in the DNA damage response pathway that also modulates inflammation (123, 124). Curiously, the ATM inhibitor reduced RSV levels while inhibitors of two other DNA damage transducers, ATR and PARP, did not affect RSV (Figure 20A). This suggests a unique role for ATM in the life cycle of RSV. Previous research has suggested that ATM and ATR may support the replication of single-stranded RNA viruses, potentially explaining the reduction in RSV levels upon ATM inhibition (125).

Interestingly, ATM inhibition not only reduced the γH2AX levels (Figure 20A), which might reflect diminished RSV replication, but also increased IL-1β release (Figure 21). This paradox suggests that while ATM typically responds to DNA damage, its inhibition may disrupt normal virus-host interactions, leading to altered inflammatory responses (123, 124). Specifically, the rise in IL-1β could result from either an increase in pro-IL-1β synthesis or a change in its processing, potentially tied to broader cellular responses like cell death or senescence under ATM-inhibited conditions (123, 124).

Future investigations should further explore the dual role of ATM in both viral replication and the inflammatory response, particularly exploring how changes in ATM activity influence pro-IL-1β processing in viral infections. Such studies would be crucial for understanding the complex interplay between virus-induced cellular damage and the host immune response, providing insights that could lead to targeted therapeutic strategies.

5.6 Mechanisms on RSV-induced IL-1β release and DNA damage induction

To illustrate the interactions and main results of our study, we have developed a schematic model (Figure 22). This model visualizes the proposed pathways through which RSV infection leads to IL-1β release and induces DNA damage. Key components of the model include the role of DNA damage response elements, and the interplay between viral mechanisms and host cellular responses observed during RSV infection in WI-38 cells.

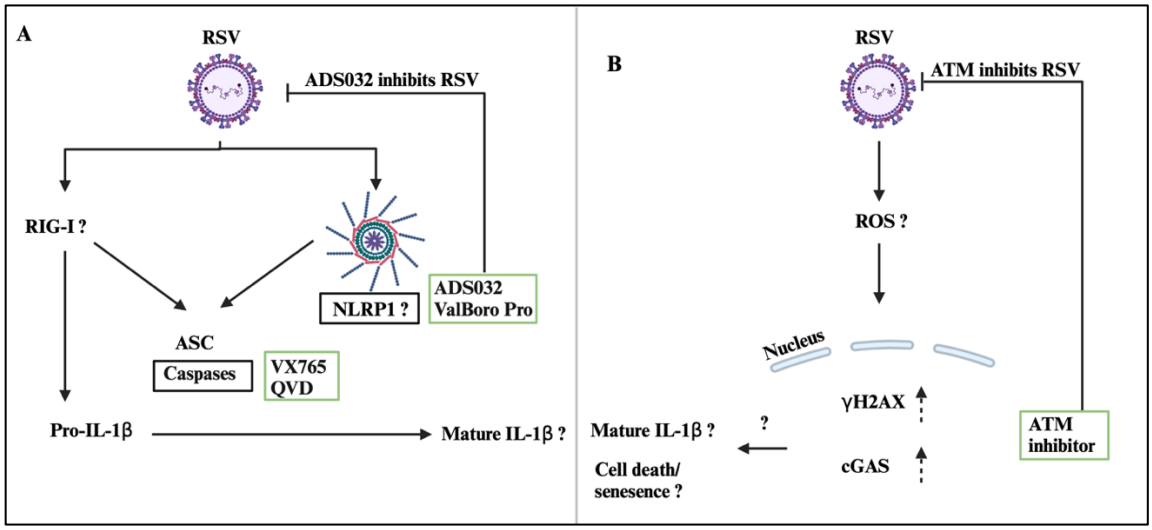

Figure 22. Proposed model for mechanisms on RSV-induced IL-1β release and DNA damage (γH2AX) induction. (A) Shows potential mechanism contributing to RSV-induced IL-1β release. **(B)** Shows potential mechanisms in RSV-induced DNA damage (γH2AX). The action point of chemical modulators applied in the study is indicated in green boxes. The process in A and B could be linked e.g. via γH2AX which could lead to caspase activation, cell death or senescence (see discussion for further details). Figure created with BioRender (www.biorender.com).

Our study explored the complex interplay between viral recognition receptors, caspase activation and inflammasome pathways in the context of RSV infection in WI-38 fibroblasts (Figure 22A). Previous studies have shown that in particularly RIG-I and TLR3 regulate inflammation in WI-38 cells infected with human metapneumovirus (126), a virus closely related to RSV. RIG-I receptors have been implicated in activating the inflammasome, leading to the production of pro-inflammatory cytokines (119). In particular, activation of RIG-I has

been linked to NF-κB-dependent induction of pro-IL-1β and subsequent inflammasome activation in bone marrow-derived dendritic cells (BMDCs) following Vesicular stomatitis virus (VSV) infection (119). This suggests a potential mechanism whereby RIG-I, upon recognizing RSV, could similarly activate the inflammasome in lung fibroblasts.

In addition to the roles of viral recognition receptors, our data suggest the significance of caspase pathways in mediating the inflammatory responses in RSV-infected WI-38 cells. The activation of these caspases may be linked to the cell death mechanisms induced by viral infection (49). The involvement of RIG-I, TLR3, and caspases in the immune response to RSV in WI-38 fibroblasts highlights potential therapeutic targets for controlling viral infections and the associated inflammatory responses (126). Modulating the activity of these molecules could offer new avenues for reducing the pathology associated with RSV and similar viral infections, potentially minimizing tissue damage and improving clinical outcomes.

Further, our findings demonstrate a significant increase in γH2AX following RSV infection in WI-38 fibroblasts, suggesting an activation of the DNA damage response potentially induced by ROS (Figure 22B). Concurrently, we observed elevated levels of the cGAS protein, which is known to be stimulated by DNA fragments resulting from damage or stress (80). These results align with studies on other viral infections, such as SARS-CoV-2, where impaired DNA repair mechanisms lead to enhanced γH2AX protein levels, and potentially exacerbating cellular stress responses (127).

γH2AX is intricately linked to cellular processes such as cell death and senescence, acting as a critical balance between these pathways (90). In our study, the use of a pan-caspase inhibitor, QVD, markedly reduced both RSV-induced γH2AX protein levels and IL-1β release (Figure 18A and B). This suggests a potential linkage through mechanisms involving γH2AX-driven senescence. This notion is supported by the hypothesis that γH2AX can induce senescence-associated inflammatory responses, including IL-1β release, a hallmark of cellular senescence observed in other viral infections such as SARS-CoV-2 (128).

The mechanisms by which RSV stimulates γH2AX remain unkown, but suggest that it may involve feedback loops between senescence and cell death. This is of interest, as cGAS has been found to be activated by DNA damage e.g. γH2AX, and to induce senescence and IL-1β

release (129-132). The exact role of cGAS, and whether it mediates RSV-induced senescence and IL-1β induction would be an interesting topic to explore in future studies.

The significance of these findings extends to the potential role of fibroblasts in severe infections, such as those caused by SARS-CoV-2, where enhanced IL-1β levels are observed (128). Despite our observations on overall low IL-1β induction levels by RSV, fibroblasts may still contribute significantly within lung tissue. The association of cell death and IL-1β release with fibrotic mechanisms and potential chronic damage underscores the importance of understanding γH2AX role in genomic instability and lung tissue damage, especially if not adequately repaired (133).

6 Conclusion

In this study, we explored cell death mechanisms and components in relation to RSV infection of WI-38 lung fibroblasts. The results indicate that RSV induces lytic cell death along with IL-1β release. NLRP1 mRNA is moderately expressed in WI-38 cells, and notably, inhibition of NLRP1 reduced both RSV-induced IL-1β secretion and RSV replication levels. Further, the pan-caspase inhibitor, QVD, reduced RSV-stimulated IL-1β, while caspase-1 inhibition did not significantly inhibit IL-1β release, suggesting the involvement of alternative inflammatory pathways. Furthermore, we did not detect active caspase-1, reinforcing the potential for non-canonical pathways in mediating IL-1β release during RSV infection. The study also highlighted a significant increase in RSV-induced γH2AX and cGAS protein levels, indicating an interplay between viral infection and host DNA damage responses. The inhibition of ATM, a key kinase in the DNA damage response, effectively modulated both RSV-induced γH2AX levels and IL-1β release and impaired viral replication, emphasizing the critical connection between DNA damage response and viral pathogenesis. Overall, our results explored cell death components implicated in RSV-infected cells.

7 References

1. Flint J, Racaniello VR, Rall GF, Hatziioannou T, Skalka AM. Principles of Virology 5. ed: John Wiley & Sons 2020.
2. Turvey SE, Broide DH. Innate immunity. J Allergy Clin Immunol. 2010;125(2 Suppl 2):S24-32.
3. Parkin J, Cohen B. An overview of the immune system. Lancet. 2001;357(9270):1777-89.
4. Lee FEH, Treanor JJ. Viral Infections. Murray and Nadel's Textbook of Respiratory Medicine. 2016:527-56.e15.
5. Fendrick AM, Monto AS, Nightengale B, Sarnes M. The economic burden of non-influenza-related viral respiratory tract infection in the United States. Arch Intern Med. 2003;163(4):487-94.
6. Leung NHL. Transmissibility and transmission of respiratory viruses. Nat Rev Microbiol. 2021;19(8):528-45.
7. Chaplin DD. Overview of the immune response. J Allergy Clin Immunol. 2010;125(2 Suppl 2):S3-23.
8. Evans SS, Repasky EA, Fisher DT. Fever and the thermal regulation of immunity: the immune system feels the heat. Nat Rev Immunol. 2015;15(6):335-49.
9. Marshall JS, Warrington R, Watson W, Kim HL. An introduction to immunology and immunopathology. Allergy, Asthma & Clinical Immunology. 2018;14(2):49.
10. Li D, Wu M. Pattern recognition receptors in health and diseases. Signal Transduction and Targeted Therapy. 2021;6(1):291.
11. Mortaz E, Adcock IM, Tabarsi P, Darazam IA, Movassaghi M, Garssen J, et al. Pattern recognitions receptors in immunodeficiency disorders. Eur J Pharmacol. 2017;808:49-56.
12. Rosendahl Huber S, van Beek J, de Jonge J, Luytjes W, van Baarle D. T cell responses to viral infections - opportunities for Peptide vaccination. Front Immunol. 2014;5:171.
13. Zhao H, Wu L, Yan G, Chen Y, Zhou M, Wu Y, et al. Inflammation and tumor progression: signaling pathways and targeted intervention. Signal Transduction and Targeted Therapy. 2021;6(1):263.
14. Kany S, Vollrath JT, Relja B. Cytokines in Inflammatory Disease. Int J Mol Sci. 2019;20(23).

15. Katze MG, He Y, Gale M. Viruses and interferon: a fight for supremacy. Nature Reviews Immunology. 2002;2(9):675-87.
16. Platanias LC. Mechanisms of type-I- and type-II-interferon-mediated signalling. Nature Reviews Immunology. 2005;5(5):375-86.
17. McNab F, Mayer-Barber K, Sher A, Wack A, O'Garra A. Type I interferons in infectious disease. Nature Reviews Immunology. 2015;15(2):87-103.
18. Newton AH, Cardani A, Braciale TJ. The host immune response in respiratory virus infection: balancing virus clearance and immunopathology. Semin Immunopathol. 2016;38(4):471-82.
19. Durbin RK, Kotenko SV, Durbin JE. Interferon induction and function at the mucosal surface. Immunol Rev. 2013;255(1):25-39.
20. Collins PL, Fearns R, Graham BS. Respiratory syncytial virus: virology, reverse genetics, and pathogenesis of disease. Curr Top Microbiol Immunol. 2013;372:3-38.
21. Shi T, McAllister DA, O'Brien KL, Simoes EAF, Madhi SA, Gessner BD, et al. Global, regional, and national disease burden estimates of acute lower respiratory infections due to respiratory syncytial virus in young children in 2015: a systematic review and modelling study. Lancet. 2017;390(10098):946-58.
22. Guy C. Mechanisms of gasdermin pore formation in response to viral sensing in human respiratory epithelial cells. 2022.
23. Kaler J, Hussain A, Patel K, Hernandez T, Ray S. Respiratory Syncytial Virus: A Comprehensive Review of Transmission, Pathophysiology, and Manifestation. Cureus. 2023;15(3):e36342.
24. Baraldi E, Bonadies L, Manzoni P. Evidence on the Link between Respiratory Syncytial Virus Infection in Early Life and Chronic Obstructive Lung Diseases. Am J Perinatol. 2020;37(S 02):S26-s30.
25. Walsh EE, Hall CB. Respiratory Syncytial Virus (RSV). Mandell, Douglas, and Bennett's Principles and Practice of Infectious Diseases. 2015:1948-60.e3.
26. Zambon MC, Stockton JD, Clewley JP, Fleming DM. Contribution of influenza and respiratory syncytial virus to community cases of influenza-like illness: an observational study. Lancet. 2001;358(9291):1410-6.
27. Nam HH, Ison MG. Respiratory syncytial virus infection in adults. BMJ. 2019;366:l5021.
28. Battles MB, McLellan JS. Respiratory syncytial virus entry and how to block it. Nature Reviews Microbiology. 2019;17(4):233-45.

29. Sun Y, López CB. The innate immune response to RSV: Advances in our understanding of critical viral and host factors. Vaccine. 2017;35(3):481-8.
30. Mogensen TH. Pathogen recognition and inflammatory signaling in innate immune defenses. Clin Microbiol Rev. 2009;22(2):240-73, Table of Contents.
31. Efstathiou C, Abidi SH, Harker J, Stevenson NJ. Revisiting respiratory syncytial virus's interaction with host immunity, towards novel therapeutics. Cell Mol Life Sci. 2020;77(24):5045-58.
32. Sedeyn K, Schepens B, Saelens X. Respiratory syncytial virus nonstructural proteins 1 and 2: Exceptional disrupters of innate immune responses. PLoS Pathog. 2019;15(10):e1007984.
33. Lambert L, Sagfors AM, Openshaw PJM, Culley FJ. Immunity to RSV in Early-Life. Front Immunol. 2014;5.
34. Ouyang Y, Liao H, Hu Y, Luo K, Hu S, Zhu H. Innate Immune Evasion by Human Respiratory Syncytial Virus. Front Microbiol. 2022;13.
35. Robledo-Aceves M, Moreno-Peregrina MJ, Velarde-Rivera F, Ascencio-Esparza E, Preciado-Figueroa FM, Caniza MA, et al. Risk factors for severe bronchiolitis caused by respiratory virus infections among Mexican children in an emergency department. Medicine (Baltimore). 2018;97(9):e0057.
36. Fulda S, Gorman AM, Hori O, Samali A. Cellular stress responses: cell survival and cell death. Int J Cell Biol. 2010;2010:214074.
37. Elmore S. Apoptosis: a review of programmed cell death. Toxicol Pathol. 2007;35(4):495-516.
38. Festjens N, Vanden Berghe T, Vandenabeele P. Necrosis, a well-orchestrated form of cell demise: Signalling cascades, important mediators and concomitant immune response. Biochimica et Biophysica Acta (BBA) - Bioenergetics. 2006;1757(9):1371-87.
39. Wei X, Xie F, Zhou X, Wu Y, Yan H, Liu T, et al. Role of pyroptosis in inflammation and cancer. Cell Mol Immunol. 2022;19(9):971-92.
40. Bergsbaken T, Fink SL, Cookson BT. Pyroptosis: host cell death and inflammation. Nat Rev Microbiol. 2009;7(2):99-109.
41. Lee E, Song CH, Bae SJ, Ha KT, Karki R. Regulated cell death pathways and their roles in homeostasis, infection, inflammation, and tumorigenesis. Exp Mol Med. 2023;55(8):1632-43.
42. Bertheloot D, Latz E, Franklin BS. Necroptosis, pyroptosis and apoptosis: an intricate game of cell death. Cell Mol Immunol. 2021;18(5):1106-21.

43. Yudhawati R, Sakina S, Fitriah M. Interleukin-1β and Interleukin-10 Profiles and Ratio in Serum of COVID-19 Patients and Correlation with COVID-19 Severity: A Time Series Study. Int J Gen Med. 2022;15:8043-54.
44. Lee K-H, Kang T-B. The Molecular Links between Cell Death and Inflammasome. Cells. 2019;8(9):1057.
45. Bedient L, Pokharel SM, Chiok KR, Mohanty I, Beach SS, Miura TA, et al. Lytic Cell Death Mechanisms in Human Respiratory Syncytial Virus-Infected Macrophages: Roles of Pyroptosis and Necroptosis. Viruses. 2020;12(9).
46. Wang Y, Qi H, Liu Y, Duan C, Liu X, Xia T, et al. The double-edged roles of ROS in cancer prevention and therapy. Theranostics. 2021;11:4839-57.
47. Van Opdenbosch N, Lamkanfi M. Caspases in Cell Death, Inflammation, and Disease. Immunity. 2019;50(6):1352-64.
48. He WT, Wan H, Hu L, Chen P, Wang X, Huang Z, et al. Gasdermin D is an executor of pyroptosis and required for interleukin-1β secretion. Cell Res. 2015;25(12):1285-98.
49. McIlwain DR, Berger T, Mak TW. Caspase functions in cell death and disease. Cold Spring Harb Perspect Biol. 2013;5(4):a008656.
50. Sagulenko V, Vitak N, Vajjhala PR, Vince JE, Stacey KJ. Caspase-1 Is an Apical Caspase Leading to Caspase-3 Cleavage in the AIM2 Inflammasome Response, Independent of Caspase-8. J Mol Biol. 2018;430(2):238-47.
51. Zhu L, Li X, Xu F, Yin Z, Jin J, Liu Z, et al. Network modeling-based identification of the switching targets between pyroptosis and secondary pyroptosis. Chaos, Solitons & Fractals. 2022;155:111724.
52. Hallé M, Liu YC, Hardy S, Théberge JF, Blanchetot C, Bourdeau A, et al. Caspase-3 regulates catalytic activity and scaffolding functions of the protein tyrosine phosphatase PEST, a novel modulator of the apoptotic response. Mol Cell Biol. 2007;27(3):1172-90.
53. Frantz S, Ducharme A, Sawyer D, Rohde LE, Kobzik L, Fukazawa R, et al. Targeted deletion of caspase-1 reduces early mortality and left ventricular dilatation following myocardial infarction. J Mol Cell Cardiol. 2003;35(6):685-94.
54. Yang X, Liu X, Nie Y, Zhan F, Zhu B. Oxidative stress and ROS-mediated cellular events in RSV infection: potential protective roles of antioxidants. Virol J. 2023;20(1):224.
55. Elesela S, Morris SB, Narayanan S, Kumar S, Lombard DB, Lukacs NW. Sirtuin 1 regulates mitochondrial function and immune homeostasis in respiratory syncytial virus infected dendritic cells. PLoS Pathog. 2020;16(2):e1008319.

56. Liao Y, Hussain T, Liu C, Cui Y, Wang J, Yao J, et al. Endoplasmic Reticulum Stress Induces Macrophages to Produce IL-1β During Mycobacterium bovis Infection via a Positive Feedback Loop Between Mitochondrial Damage and Inflammasome Activation. Front Immunol. 2019;10.
57. Noh SS, Shin HJ. RSV Induces Activation of Intracellular EGFR on the Mitochondrial Membrane for Virus Propagation. International Journal of Molecular Sciences. 2023;24(24):17431.
58. Cerato JA, da Silva EF, Porto BN. Breaking Bad: Inflammasome Activation by Respiratory Viruses. Biology. 2023;12(7):943.
59. Martinon F, Burns K, Tschopp J. The inflammasome: a molecular platform triggering activation of inflammatory caspases and processing of proIL-beta. Mol Cell. 2002;10(2):417-26.
60. de Zoete MR, Palm NW, Zhu S, Flavell RA. Inflammasomes. Cold Spring Harb Perspect Biol. 2014;6(12):a016287.
61. Christgen S, Place DE, Kanneganti TD. Toward targeting inflammasomes: insights into their regulation and activation. Cell Res. 2020;30(4):315-27.
62. Finger JN, Lich JD, Dare LC, Cook MN, Brown KK, Duraiswami C, et al. Autolytic proteolysis within the function to find domain (FIIND) is required for NLRP1 inflammasome activity. J Biol Chem. 2012;287(30):25030-7.
63. Barry K, Murphy C, Mansell A. NLRP1- A CINDERELLA STORY: a perspective of recent advances in NLRP1 and the questions they raise. Communications Biology. 2023;6(1):1274.
64. Chavarría-Smith J, Vance RE. The NLRP1 inflammasomes. Immunol Rev. 2015;265(1):22-34.
65. Zhou JY, Sarkar MK, Okamura K, Harris JE, Gudjonsson JE, Fitzgerald KA. Activation of the NLRP1 inflammasome in human keratinocytes by the dsDNA mimetic poly(dA:dT). Proc Natl Acad Sci U S A. 2023;120(5):e2213777120.
66. Okondo MC, Johnson DC, Sridharan R, Go EB, Chui AJ, Wang MS, et al. DPP8 and DPP9 inhibition induces pro-caspase-1-dependent monocyte and macrophage pyroptosis. Nat Chem Biol. 2017;13(1):46-53.
67. Hollingsworth LR, Sharif H, Griswold AR, Fontana P, Mintseris J, Dagbay KB, et al. DPP9 sequesters the C terminus of NLRP1 to repress inflammasome activation. Nature. 2021;592(7856):778-83.

68. Bulté D, Rigamonti C, Romano A, Mortellaro A. Inflammasomes: Mechanisms of Action and Involvement in Human Diseases. Cells. 2023;12(13):1766.
69. Wang Z, Zhang S, Xiao Y, Zhang W, Wu S, Qin T, et al. NLRP3 Inflammasome and Inflammatory Diseases. Oxid Med Cell Longev. 2020;2020:4063562.
70. Blevins HM, Xu Y, Biby S, Zhang S. The NLRP3 Inflammasome Pathway: A Review of Mechanisms and Inhibitors for the Treatment of Inflammatory Diseases. Front Aging Neurosci. 2022;14:879021.
71. Xu J, Núñez G. The NLRP3 inflammasome: activation and regulation. Trends Biochem Sci. 2023;48(4):331-44.
72. Van Opdenbosch N, Gurung P, Vande Walle L, Fossoul A, Kanneganti T-D, Lamkanfi M. Activation of the NLRP1b inflammasome independently of ASC-mediated caspase-1 autoproteolysis and speck formation. Nature Communications. 2014;5(1):3209.
73. Abderrazak A, Syrovets T, Couchie D, El Hadri K, Friguet B, Simmet T, et al. NLRP3 inflammasome: from a danger signal sensor to a regulatory node of oxidative stress and inflammatory diseases. Redox Biol. 2015;4:296-307.
74. Bauernfeind FG, Horvath G, Stutz A, Alnemri ES, MacDonald K, Speert D, et al. Cutting edge: NF-kappaB activating pattern recognition and cytokine receptors license NLRP3 inflammasome activation by regulating NLRP3 expression. J Immunol. 2009;183(2):787-91.
75. Franchi L, Eigenbrod T, Núñez G. Cutting edge: TNF-alpha mediates sensitization to ATP and silica via the NLRP3 inflammasome in the absence of microbial stimulation. J Immunol. 2009;183(2):792-6.
76. Chen Q, Sun L, Chen ZJ. Regulation and function of the cGAS–STING pathway of cytosolic DNA sensing. Nat Immunol. 2016;17(10):1142-9.
77. Iampietro M, Dumont C, Mathieu C, Spanier J, Robert J, Charpenay A, et al. Activation of cGAS/STING pathway upon paramyxovirus infection. iScience. 2021;24(6):102519.
78. Neufeldt CJ, Cerikan B, Cortese M, Frankish J, Lee JY, Plociennikowska A, et al. SARS-CoV-2 infection induces a pro-inflammatory cytokine response through cGAS-STING and NF-κB. Commun Biol. 2022;5(1):45.
79. Sun L, Wu J, Du F, Chen X, Chen ZJ. Cyclic GMP-AMP synthase is a cytosolic DNA sensor that activates the type I interferon pathway. Science. 2013;339(6121):786-91.

80. Decout A, Katz JD, Venkatraman S, Ablasser A. The cGAS–STING pathway as a therapeutic target in inflammatory diseases. Nature Reviews Immunology. 2021;21(9):548-69.
81. Dvorkin S, Cambier S, Volkman HE, Stetson DB. New frontiers in the cGAS-STING intracellular DNA-sensing pathway. Immunity. 2024;57(4):718-30.
82. Liu J, Zhou J, Luan Y, Li X, Meng X, Liao W, et al. cGAS-STING, inflammasomes and pyroptosis: an overview of crosstalk mechanism of activation and regulation. Cell Communication and Signaling. 2024;22(1):22.
83. Zheng W, Liu A, Xia N, Chen N, Meurens F, Zhu J. How the Innate Immune DNA Sensing cGAS-STING Pathway Is Involved in Apoptosis. Int J Mol Sci. 2023;24(3).
84. Skopelja-Gardner S, An J, Elkon KB. Role of the cGAS-STING pathway in systemic and organ-specific diseases. Nat Rev Nephrol. 2022;18(9):558-72.
85. Firsanov DV, Solovjeva LV, Svetlova MP. H2AX phosphorylation at the sites of DNA double-strand breaks in cultivated mammalian cells and tissues. Clin Epigenetics. 2011;2(2):283-97.
86. Rogakou EP, Pilch DR, Orr AH, Ivanova VS, Bonner WM. DNA Double-stranded Breaks Induce Histone H2AX Phosphorylation on Serine 139 *. J Biol Chem. 1998;273(10):5858-68.
87. Lu C, Zhu F, Cho YY, Tang F, Zykova T, Ma WY, et al. Cell apoptosis: requirement of H2AX in DNA ladder formation, but not for the activation of caspase-3. Mol Cell. 2006;23(1):121-32.
88. Yang J, Yu Y, Hamrick HE, Duerksen-Hughes PJ. ATM, ATR and DNA-PK: initiators of the cellular genotoxic stress responses. Carcinogenesis. 2003;24(10):1571-80.
89. Kurz EU, Lees-Miller SP. DNA damage-induced activation of ATM and ATM-dependent signaling pathways. DNA Repair (Amst). 2004;3(8-9):889-900.
90. Prabhu KS, Kuttikrishnan S, Ahmad N, Habeeba U, Mariyam Z, Suleman M, et al. H2AX: A key player in DNA damage response and a promising target for cancer therapy. Biomed Pharmacother. 2024;175:116663.
91. Schütz CS, Stope MB, Bekeschus S. H2A.X Phosphorylation in Oxidative Stress and Risk Assessment in Plasma Medicine. Oxid Med Cell Longev. 2021;2021:2060986.
92. Muresanu C, Somasundaram SG, Vissarionov SV, Torres Solis LF, Solís Herrera A, Kirkland CE, et al. Updated Understanding of Cancer as a Metabolic and Telomere-Driven Disease, and Proposal for Complex Personalized Treatment, a Hypothesis. International Journal of Molecular Sciences. 2020;21(18):6521.

93. ThermoFisher. The Basics of Fetal Bovine Serum Use in Cell Culture [cited 2024 8. feb]. Available from: https://www.thermofisher.com/no/en/home/references/gibco-cell-culture-basics/cell-culture-environment/culture-media/fbs-basics.html.
94. Kurreck J, Stein CA. Molecular Medicine: An Introduction: Wiley; 2016.
95. Jakobs C, Bartok E, Kubarenko A, Bauernfeind F, Hornung V. Immunoblotting for active caspase-1. Methods Mol Biol. 2013;1040:103-15.
96. Rajan A, Piedra FA, Aideyan L, McBride T, Robertson M, Johnson HL, et al. Multiple Respiratory Syncytial Virus (RSV) Strains Infecting HEp-2 and A549 Cells Reveal Cell Line-Dependent Differences in Resistance to RSV Infection. J Virol. 2022;96(7):e0190421.
97. Yashiro T, Yamamoto M, Araumi S, Hara M, Yogo K, Uchida K, et al. PU.1 and IRF8 Modulate Activation of NLRP3 Inflammasome via Regulating Its Expression in Human Macrophages. Front Immunol. 2021;12.
98. Segovia J, Sabbah A, Mgbemena V, Tsai SY, Chang TH, Berton MT, et al. TLR2/MyD88/NF-κB pathway, reactive oxygen species, potassium efflux activates NLRP3/ASC inflammasome during respiratory syncytial virus infection. PLoS One. 2012;7(1):e29695.
99. Al Hamrashdi M, Brady G. Regulation of IRF3 activation in human antiviral signaling pathways. Biochem Pharmacol. 2022;200:115026.
100. Shi W, Jin M, Chen H, Wu Z, Yuan L, Liang S, et al. Inflammasome activation by viral infection: mechanisms of activation and regulation. Front Microbiol. 2023;14:1247377.
101. Kondo T, Kinouchi H, Kawase M, Yoshimoto T. Differential response in the release of hydrogen peroxide between astroglial cells and endothelial cells following hypoxia/reoxygenation. Neurosci Lett. 1996;215(2):103-6.
102. Victorelli S, Salmonowicz H, Chapman J, Martini H, Vizioli MG, Riley JS, et al. Apoptotic stress causes mtDNA release during senescence and drives the SASP. Nature. 2023;622(7983):627-36.
103. Yu Y, Xu L, Qi L, Wang C, Xu N, Liu S, et al. ABT737 induces mitochondrial pathway apoptosis and mitophagy by regulating DRP1-dependent mitochondrial fission in human ovarian cancer cells. Biomed Pharmacother. 2017;96:22-9.
104. England H, Summersgill HR, Edye ME, Rothwell NJ, Brough D. Release of interleukin-1α or interleukin-1β depends on mechanism of cell death. J Biol Chem. 2014;289(23):15942-50.

105. Yao J, Sterling K, Wang Z, Zhang Y, Song W. The role of inflammasomes in human diseases and their potential as therapeutic targets. Signal Transduction and Targeted Therapy. 2024;9(1):10.
106. Docherty CA, Fernando AJ, Rosli S, Lam M, Dolle RE, Navia MA, et al. A novel dual NLRP1 and NLRP3 inflammasome inhibitor for the treatment of inflammatory diseases. Clin Transl Immunology. 2023;12(6):e1455.
107. Lee D-J, Du F, Chen S-W, Nakasaki M, Rana I, Shih VFS, et al. Regulation and Function of the Caspase-1 in an Inflammatory Microenvironment. J Invest Dermatol. 2015;135(8):2012-20.
108. Morgan CW, Diaz JE, Zeitlin SG, Gray DC, Wells JA. Engineered cellular gene-replacement platform for selective and inducible proteolytic profiling. Proceedings of the National Academy of Sciences. 2015;112(27):8344-9.
109. Rogakou EP, Nieves-Neira W, Boon C, Pommier Y, Bonner WM. Initiation of DNA Fragmentation during Apoptosis Induces Phosphorylation of H2AX Histone at Serine 139*. J Biol Chem. 2000;275(13):9390-5.
110. Peng Y, Yang Y, Li Y, Shi T, Xu N, Liu R, et al. Mitochondrial (mt)DNA–cyclic GMP–AMP synthase (cGAS)–stimulator of interferon genes (STING) signaling promotes pyroptosis of macrophages via interferon regulatory factor (IRF)7/IRF3 activation to aggravate lung injury during severe acute pancreatitis. Cell Mol Biol Lett. 2024;29(1):61.
111. Kanarek N, Grivennikov SI, Leshets M, Lasry A, Alkalay I, Horwitz E, et al. Critical role for IL-1β in DNA damage-induced mucositis. Proc Natl Acad Sci U S A. 2014;111(6):E702-11.
112. Unterholzner L, Dunphy G. cGAS-independent STING activation in response to DNA damage. Mol Cell Oncol. 2019;6(4):1558682.
113. Cimprich KA, Li G-M, Demaria S, Gekara NO, Zha S, Chen Q. The crosstalk between DNA repair and immune responses. Mol Cell. 2023;83(20):3582-7.
114. Aki T, Uemura K. Cell Death and Survival Pathways Involving ATM Protein Kinase. Genes (Basel). 2021;12(10).
115. Matsuoka S, Ballif BA, Smogorzewska A, McDonald ER, Hurov KE, Luo J, et al. ATM and ATR Substrate Analysis Reveals Extensive Protein Networks Responsive to DNA Damage. Science. 2007;316(5828):1160-6.
116. Caron M-C, Sharma AK, O'Sullivan J, Myler LR, Ferreira MT, Rodrigue A, et al. Poly(ADP-ribose) polymerase-1 antagonizes DNA resection at double-strand breaks. Nature Communications. 2019;10(1):2954.

117. Malinczak CA, Schuler CF, Duran AJ, Rasky AJ, Mire MM, Núñez G, et al. NLRP3-Inflammasome Inhibition during Respiratory Virus Infection Abrogates Lung Immunopathology and Long-Term Airway Disease Development. Viruses. 2021;13(4).
118. Leszczyńska K, Jakubczyk D, Górska S. The NLRP3 inflammasome as a new target in respiratory disorders treatment. Front Immunol. 2022;13:1006654.
119. Poeck H, Bscheider M, Gross O, Finger K, Roth S, Rebsamen M, et al. Recognition of RNA virus by RIG-I results in activation of CARD9 and inflammasome signaling for interleukin 1 beta production. Nat Immunol. 2010;11(1):63-9.
120. Saresella M, La Rosa F, Piancone F, Zoppis M, Marventano I, Calabrese E, et al. The NLRP3 and NLRP1 inflammasomes are activated in Alzheimer's disease. Mol Neurodegener. 2016;11(1):23.
121. Sayan M, Mossman BT. The NLRP3 inflammasome in pathogenic particle and fibre-associated lung inflammation and diseases. Part Fibre Toxicol. 2016;13(1):51.
122. Walsh MP, Duncan B, Larabee S, Krauss A, Davis JP, Cui Y, et al. Val-boroPro accelerates T cell priming via modulation of dendritic cell trafficking resulting in complete regression of established murine tumors. PLoS One. 2013;8(3):e58860.
123. Shiloh Y. The ATM-mediated DNA-damage response: taking shape. Trends Biochem Sci. 2006;31(7):402-10.
124. Foley JF. ATM and Inflammation. Science Signaling. 2009;2(83):ec265-ec.
125. Li P, Xu C, Zhang X, Cao C, Wang X, Cai G. Single-stranded RNA viruses activate and hijack host apical DNA damage response kinases for efficient viral replication. Genome Instab Dis. 2022;3(2):83-7.
126. Li Y, Lund C, Nervik I, Loevenich S, Døllner H, Anthonsen MW, et al. Characterization of signaling pathways regulating the expression of pro-inflammatory long form thymic stromal lymphopoietin upon human metapneumovirus infection. Sci Rep. 2018;8(1):883.
127. Gioia U, Tavella S, Martínez-Orellana P, Cicio G, Colliva A, Ceccon M, et al. SARS-CoV-2 infection induces DNA damage, through CHK1 degradation and impaired 53BP1 recruitment, and cellular senescence. Nat Cell Biol. 2023;25(4):550-64.
128. Lee S, Yu Y, Trimpert J, Benthani F, Mairhofer M, Richter-Pechanska P, et al. Virus-induced senescence is a driver and therapeutic target in COVID-19. Nature. 2021;599(7884):283-9.
129. Li Q, Wu P, Du Q, Hanif U, Hu H, Li K. cGAS-STING, an important signaling pathway in diseases and their therapy. MedComm (2020). 2024;5(4):e511.

130. Dou Z, Ghosh K, Vizioli MG, Zhu J, Sen P, Wangensteen KJ, et al. Cytoplasmic chromatin triggers inflammation in senescence and cancer. Nature. 2017;550(7676):402-6.
131. Glück S, Guey B, Gulen MF, Wolter K, Kang TW, Schmacke NA, et al. Innate immune sensing of cytosolic chromatin fragments through cGAS promotes senescence. Nat Cell Biol. 2017;19(9):1061-70.
132. Yang H, Wang H, Ren J, Chen Q, Chen ZJ. cGAS is essential for cellular senescence. Proc Natl Acad Sci U S A. 2017;114(23):E4612-e20.
133. Wynn TA, Ramalingam TR. Mechanisms of fibrosis: therapeutic translation for fibrotic disease. Nat Med. 2012;18(7):1028-40.

Supplementary

S.1 Primer sequences

Table S1. Primer sequences for RT-qPCR

Gene	Forward (5'-3')	Reverse (5'-3')
NLRP1	ACGTTGGCCACTTGGGATCA	TGAAGGTACGGCTATGCGGG
NLRP3	TGATGTTCTGTGAAGTGCTGAA	CGCACTTTTTGTCTCATAATGA
GAPDH	hGAAGGTGAAGGTCGGAGTC	GAAGATGGTGATGGGATTTC

Table S2. Primary antibodies used for western blot

Antibody	Source/isotype	Dilution	Manufacturer
NLRP3 (D4D8T)	Rabbit	1:1000	Cell Signaling Technology (#15101)
NLRP1/NALP1	Sheep	1:400	R&D systems (#AF6788)
IL-1β	Mouse	1:1000	Cell Signaling Technology (#12242)
Caspase-1 (D7F10)	Rabbit	1:1000	Cell Signaling Technology (#3866)
Caspase-3 p20 (N-19)	Goat	1:1000	Santa Cruz (#SC-1226)
p-IRF3 (Ser396)	Rabbit	1:1000	Cell Signaling Technology (#4947)
IRF3	Rabbit	1:1000	Cell Signaling Technology (#4302)
p-STING (Ser366)	Rabbit	1:1000	Cell Signaling Technology (#50907)
STING	Rabbit	1:2000	Cell Signaling Technology (#13647)
cGAS	Rabbit	1:1000	Cell Signaling Technology (#15102)
γH2AX (Anti-phospho-Histone H2A.X (Ser139), clone JBW301)	Mouse	1:1000	Sigma (Millipore) (#05-636)
H3K9me3 (Anti-Histone H3 antibody)	Rabbit	1:1000	Abcam (#AB1791)
p-TBK-1/NAK (Ser172)	Rabbit	1:1000	Cell Signaling Technology (#5483)

TBK-1/NAK	Rabbit	1:1000	Cell Signaling Technology (#3013)
p-NF-kB-P65 (Ser536)	Rabbit	1:1000	Cell Signaling Technology (#3033)
NF-kB-P65	Rabbit	1:1000	Cell Signaling Technology (#8242)
RSV (2F7)	Mouse	1:500	Novusbio (NB110-37246)
GAPDH	Rabbit	1:10 000	Cell Signaling Technology (#5174)

Table S3. Secondary antibodies used for western blot

Antibody	Source/isotype	Immunogen	Dilution	Manufacturer
IRDye ® GAR680RD	Goat IgG	Rabbit IgG	1:20 00	LI-COR Biosciences (#926-68071)
IRDye ® GAM680RD	Goat IgG	Mouse IgG	1:20 000	LI-COR Biosciences (#926-68070)
IRDye® GAR800CW	Goat IgG	Rabbit IgG	1:5000	LI-COR Biosciences (#926-32211)
IRDye ® GAM800CW	Goat IgG	Mouse IgG	1:5000	LI-COR Biosciences (#926-32210)
DyLight ™ RAS800	Rabbit IgG	Sheep IgG	1:10 000	Thermo Fisher Scientific (#SA5-10060)

S.2 Buffers and wash solutions

1% Lysis buffer was used to lyse the cells prior to Western blot analysis. The components used in 1% lysis buffer is shown in Table S4. The components required to prepare the TBST and TBS wash buffers are listed in Table S5.

Table S4. Components in 1% lysis buffer. dH2O is added to a total volume of 500ul.

Compound	Volume
Tris [1M]	25
NaCl [1M]	75
Glycerol	50
Triton X-100	5
EDTA [0.5M]	2

Table S5. Components required to prepare the TBST and TBS wash buffers, dissolved in MQ water to a final volume of 1 liter.

Compound	TBS	TBST
NaCl	88g	88g
Tris-HCL [1M] (pH 7.5)	100 ml	100 ml
Tween 20		10 ml

S.3 Western blot analysis revealed undetectable levels of NLRP3 protein in RSV-infected HEp-2 cells.

RSV-infected HEp-2 cells at 12-, 24-, 36-, 48-, 60- and 72-hours, with a multiplicity of infection (MOI) of 3. TNF-α and Nigericin was used as controls. The NLRP3 antibody detect protein bands at 110 kDa, but no bands were detected (Figure 23).

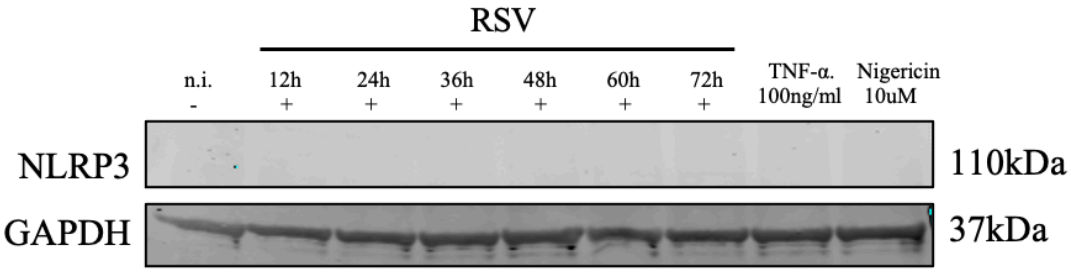

Figure 23. NLRP3 is not expressed in RSV-infected HEp-2 cells. HEp-2 cells were infected with a multiplicity of infection (MOI) of 3 for time points ranging from 12-72 hours. Tumor necrosis factor-alpha (TNF-α) at a concentration of 100 ng/ml for 48 hours. Nigericin, applied at a concentration of 10 μM for 2 hours. The presented data is compiled from one kinetic experiment. The expected molecular weights for the detected proteins are indicated in kilodaltons (kDa).

S.4 Table of C_T mean values from RT-qPCR analysis of NLRP1 and NLRP3 in resting cells.

Ct values between 16-29 indicates a moderate amount of target nucleic acid. Ct mean values ranging from 30-35 indicates a low amount of target nucleic acid, whereas Ct mean values above 35 suggested that the target is near the limit of detection, potentially rendering results unreliable (Table S6).

NLRP1	C_T Mean	C_T Mean GAPDH
NHDF	29,78	19,78
WI-38	29,19	19,22

MDM	30,61	20,16
PBMCs	25,87	21,72
A549	35,96	18,91
NECs	27,84	19,70
HEp-2	34,26	18,80
NLRP3	**C_T Mean**	**C_T Mean GAPDH**
NHDF	34,08	19,78
WI-38	29,04	19,22
MDM	23,39	20,16
PBMCs	21,33	21,72
A549	37,22	18,91
NECs	27,44	19,70
HEp-2	Undetermined	18,80

Table S6. Results from a quantitative PCR (qPCR) analysis utilizing primers for NLRP1 and NLRP3 across various cell lines. Ct values between 16-29 indicating a moderate amount of target nucleic acid. Ct values ranging from 30-35 were indicative of a low amount of target nucleic acid, whereas Ct values above 35 suggested that the target is near the limit of detection, potentially rendering results unreliable. GAPDH served as housekeeping genes to ensure rigorous normalization of gene expression across the assessed cell lines.

S.5 Active caspase-1 western blot

To determine whether RSV triggers inflammasome activation through caspase-1 activation, we analyzed active caspase-1 in the supernatant of WI-38 cells by using western blot analysis. Unfortunately, the results showed that protein migration was likely distorted by fetal bovine serum (FBS) in medium and it was not possible to relate any protein bands to molecular weight size and to detect active caspase-1 (Figure 24).

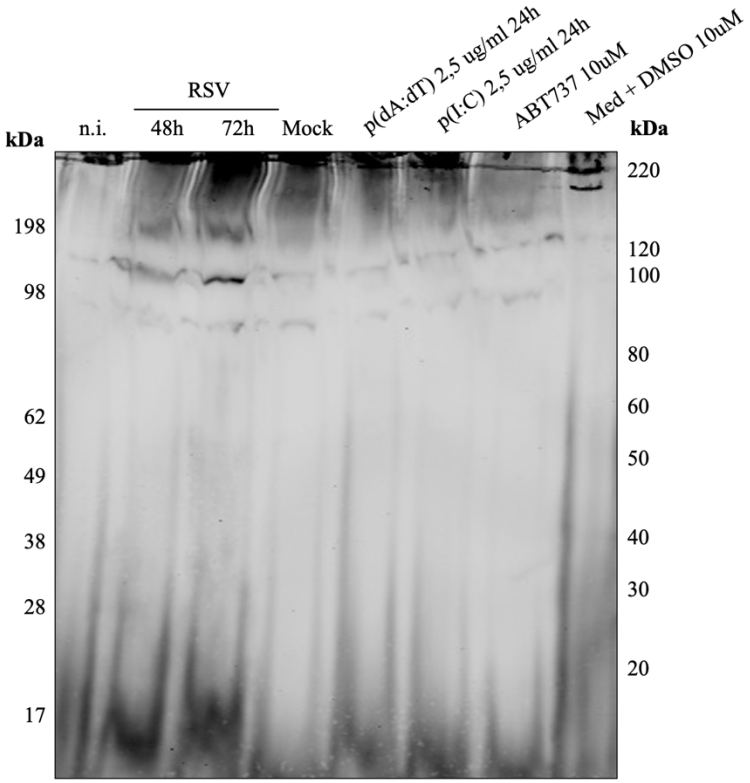

Figure 24. Active caspase-1 western blot. When trying to detect active caspase-1, it shows that protein migration was likely distorted by fetal bovine serum (FBS) in medium and it was not possible to relate any bands to molecular weight size and to detect active caspase-1. Molecular weight for See Blue ladder (to the left) and Magic Mark ladder (to the right) indicated in kDa. One experiment with two biological replicates showed the same.

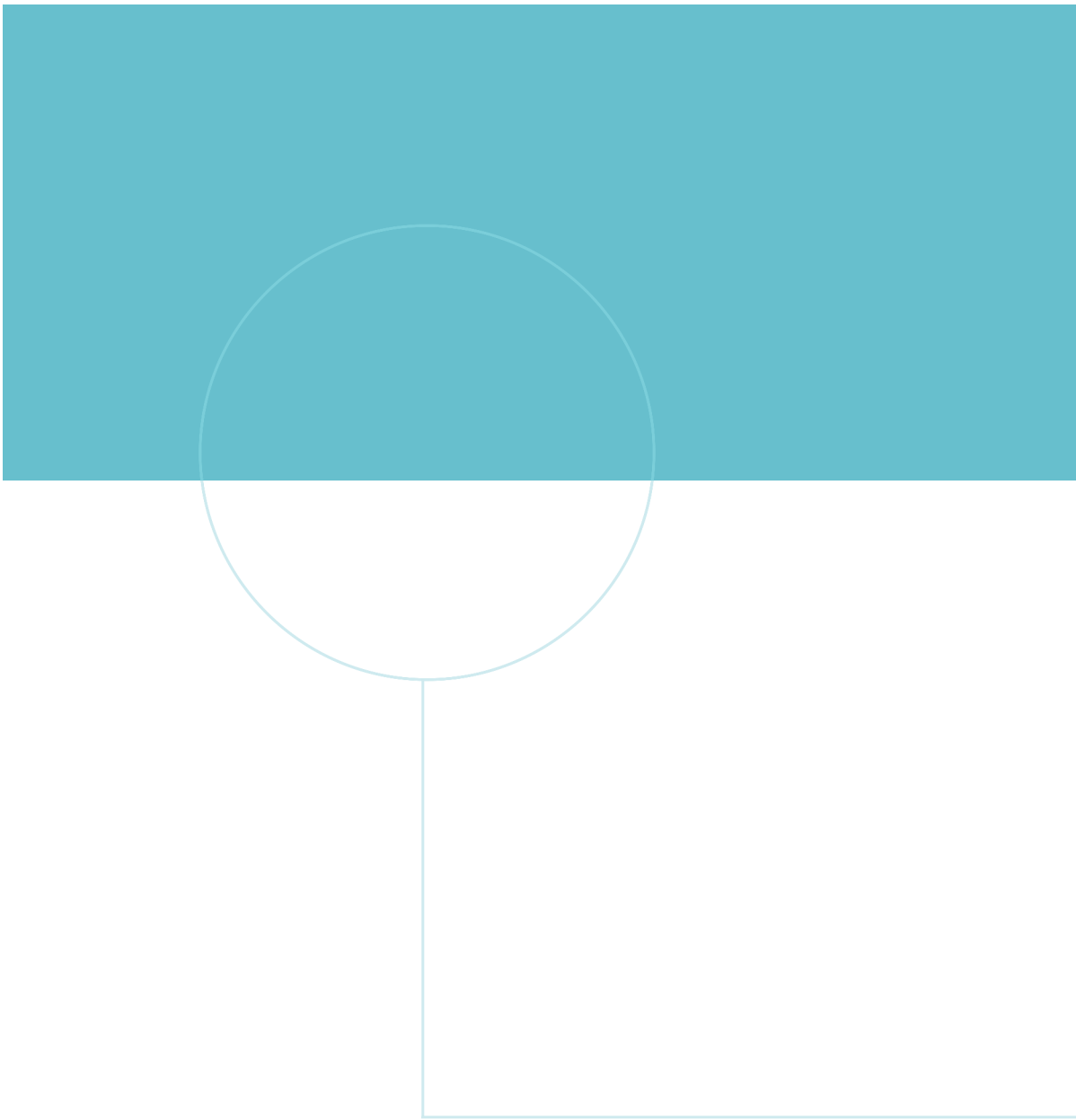

NTNU

Norwegian University of
Science and Technology